Spatial variability of the sources and distribution of fluoride in groundwater of the Sanya alluvial plain aquifers in northern Tanzania

Julian Ijumulana, Fanuel Ligate, Regina Irunde, Prosun Bhattacharya, Arslan Ahmad, Ines Tomašek, Jyoti Prakash Maity, Felix Mtalo

PII: S0048-9697(21)07229-6

DOI: https://doi.org/10.1016/j.scitotenv.2021.152153

Reference: STOTEN 152153

To appear in: *Science of the Total Environment*

Received date: 15 July 2021

Revised date: 1 November 2021

Accepted date: 29 November 2021

Please cite this article as: J. Ijumulana, F. Ligate, R. Irunde, et al., Spatial variability of the sources and distribution of fluoride in groundwater of the Sanya alluvial plain aquifers in northern Tanzania, *Science of the Total Environment* (2021), https://doi.org/10.1016/j.scitotenv.2021.152153

Spatial variability of the sources and distribution of fluoride in groundwater of the Sanya alluvial plain aquifers in northern Tanzania

Julian Ijumulana [a, b, c, *], Fanuel Ligate [a, b, d], Regina Irunde [a, b, e], Prosun Bhattacharya [a, f], Arslan Ahmad [a, g], Ines Tomašek [h,i], Jyoti Prakash Maity [j], Felix Mtalo [b]

[a]*KTH-International Groundwater Arsenic Research Group, Department of Sustainable Development, Environmental Science and Engineering, KTH Royal Institute of Technology, Teknikringen 10B, SE-100 44 Stockholm, Sweden.*

[b]*Department of Water Resources Engineering, College of Engineering and Technology, University of Dar es Salaam, Dar es Salaam, Tanzania.*

[c]*Department of Transportation and Geotechnical Engineering, College of Engineering and Technology, University of Dar es Salaam, Dar es Salaam, Tanzania.*

[d]*Department of Chemistry, Mkwawa College of Education, University of Dar es Salaam, Tanzania.*

[e]*Department of Chemistry, College of Natural and Applied Sciences, University of Dar es Salaam, Tanzania.*

[f]*KWR Water cycle Research Institute, Groningenhaven 7, 3433 PE Nieuwegein, The Netherlands*

[g]*SIBELCO Ankerpoort NV, Op de Bos 300, 6223 EP Maastricht, The Netherlands.*

[h]*Laboratoire Magmas et Volcans (LMV), CNRS, IRD, OPGC, Université Clermont Auvergne, Clermont-Ferrand, France.*

[i]*Institute of Genetic Reproduction and Development (iGReD), Translational Approach to Epithelial Injury and Repair Team, CNRS UMR 6293, INSERM U1103, Université Clermont Auvergne, Clermont-Ferrand, France.*

[j]*Department of Chemistry, School of Applied Sciences, KIIT Deemed to be University, Bhubaneswar, Odisha 751024, India.*

**corresponding author: julianij@kth.se; ijumulanajulian@gmail.com*

Abstract

Groundwater contamination from geogenic sources poses challenges to many countries, especially in the developing world. In Tanzania, the elevated fluoride (F^-) concentration and related chronic fluorosis associated with drinking F^- rich water are common in the East African Rift Valley regions. In these regions, F^- concentration is space dependence which poses much uncertainty when targeting safe source for drinking water. To account for the spatial effects, intergrated exploratory spatial data analysis , regression analysis, and geographical information systems tools were used to associate the distribution of F^- in groundwater with spatial variability in terrain slopes, volcanic deposits, recharge water/vadose materials contact time, groundwater resource developmentfor irrigated agriculture in the Sanya alluvial plain (SAP) of northern Tanzania. The F^- concentration increased with distance from steep slopes where the high scale of variation was recorded in the gentle sloping and flat grounds within the SAP. The areas covered with debris avalanche deposits in the gentle sloping and flat grounds correlated with the high spatial variability in F^- concentration. Furthermore, the high spatial variability in F^- correlated positively with depth to groundwater in the Sanya flood plain. In contrast, a negative correlation between F^- and borehole depth was observed. The current irrigation practices in the Sanya alluvial plain contribute to the high spatial variability in F^- concentration, particularly within the perched shallow aquifers in the volcanic river valleys. The findings of this study are important to the overall chain of safe water supply process in historically fluorotic regions. They provide new insights into the well-known F^- contamination through the use of modern geospatial methods and technologies. In Tanzania's context, the findings can improve the current process of drilling permits issuance by the authority and guide the local borehole drillers to be precise in siting safe source for drinking water.

Keywords: Fluoride contamination**,** volcanic deposits, Spatial variability, Geospatial analysis, Sanya alluvial plain, Northern Tanzania.

1. Introduction

Access to a safe and sustainable water source for various uses is a prerequisite to humankind. In African countries experiencing the arid and semi-arid type of climates, groundwater remains a sustainable source of water to meet demand from households domestic use, livestock, irrigation and, industry (Cobbing and Hiller, 2019; Gaye and Tindimugaya, 2019; Ligate et al., 2021; MacDonald and Calow, 2009; Pavelic et al., 2012). However, high concentration of F^- and other potentially toxic elements of health concerns have rendered many groundwater sources unsuitable for drinking purpose (Fawell and Nieuwenhuijsen, 2003; Tomašek et al., 2021; Kimambo et al., 2019; Ligate et al., 2021; WHO, 2011).

Despite F^- is an essential element for the proper development of human organs in the range of 0.5 to 1.5 mg/L in drinking water (WHO, 2011), the consumption of F^- above or below the recommended range over a long period may cause dental caries, fluorosis, and other non-carcinogenic health problems (Dissanayake, 1991; Mohanta and Mohanty, 2018; Shivaprakash, et al., 2011; Susheela and Bhatnagar, M., 2002). Exposure to high levels of F^- has effects across all age groups with increased severity on children as it can cause reduced intelligent quotient (Bhattacharya et al., 2020; Mridha et al., 2021; Shivaprakash et al., 2011).

Dental caries, fluorosis, and other health problems emanating from consuming F^- contaminated food and water have been reported in many parts of the world (Kimambo et al., 2019; Mohanta and Mohanty, 2018). In northern development zone (NDZ) of Tanzania, low to high risk zones in terms of dental caries and fluorosis have been reported within the East African Rift Valley (EARV) graben and around the major stratovolcanoes (Ijumulana et al., 2020, 2021). Usually, both geogenic and anthropogenic sources trigger the flux of F^- leading to contamination of groundwater systems across the world. While the anthropogenic sources are caused by human development activities, the geogenic sources occur naturally through the process of water and rock/soil/sediment interactions leading to the release of F^- in substantial amounts through dissolution of F^- bearing minerals (Bretzler and Johnson, 2015; Brindha and Elango,

2011; Chowdhury et al., 2019; Jacks et al., 2005; Kimambo et al., 2019; Maity et al., 2021; Vithanage and Bhattacharya, 2015).

Groundwater contamination by F^- from geogenic sources in the African continent is controlled by natural conditions of the local geological and hydrogeological setting together with climatic conditions (Gaye and Tindimugaya, 2019; MacDonald and Calow, 2009). Four hydrogeological environments exist in the African continent hosting substantial groundwater for various purposes mainly in ruraland a significant portion in urban and peri-urban settings (MacDonald et al., 2012). In Tanzania, especially in the NDZ, which lies within the EARV, potential groundwater is hosted in the complex hydrogeological environments of sedimentary, metamorphic, and volcanic origin. Like in many parts of the Sub-Saharan African (SSA) hydrogeological settings, the shallow nature of the depth to groundwater (0-25 m below ground level) encourages easy and affordable access to groundwater reservoirs (MacDonald et al., 2012). The methods of accessibility to groundwater, include hand-dug wells, machine dug wells, boreholes, and springs (Water Quality Service Division, 2016).

Although groundwater is of high socio-economic and ecological importance, and an important strategic resource throughout SSA, spatial data on groundwater systems are sparse or even absent resulting in limited insights on its current state at a local scale (Adelana and Macdonald, 2008; MacDonald et al., 2012; Lapworth et al., 2020). Spatial data, in the context of groundwater studies,refer to quantitative and qualitative information on the status of its quantity and quality for different uses. The absence of spatial data is a serious limitation for sustainable development and management of groundwater resources. However, efforts to improve the situation have been made through the publication of syntheses and reviews at the national, regional, and continental levels over the last decade (Braune and Xu, 2008; Gaye and Tindimugaya, 2019; GW·MATE, 2011; Ijumulana et al., 2020; Pavelic et al., 2012; MacDonald et al., 2012). Given that the geogenic contaminated groundwater in the volcanic areas of the EARV occurs in heterogeneous hydrogeological environments, inadequate insights about the geomorphology, climate, unsaturated surface materials, aquifer properties and the methods used to access groundwater can lead to targeting the unsafe source of drinking water (Pavelic et al., 2012).

This study highlights the need and application of modern geospatial methods and technologies to understand the distribution of F^- and processes triggering its spatial variability in groundwater systems. Specifically, exploratory spatial data analysis (ESDA) methods, ordinary least squares (OLS) regression modeling, and Geographical Information Systems (GIS) were used to assess the effects of spatial variability in terrain slopes, depth to groundwater, borehole depth, screening depth, groundwater level and irrigated agricultural practices on the widespread of F^- concentration in groundwater sources used for drinking purpose. The case study area was the Sanya alluvial plain, which is part of the regional F^- contamination hotspot in northern Tanzania (Ijumulana et al., 2020; 2021).

1.1 The study area

1.1.1 General description

This study was conducted within the Sanya alluvial plain (SAP) that originates at the boundary between the Internal and Pangani drainage basin (Fig. 1). The SAP extends southwards between the southeastern and southwestern slopes of Mt. Meru and Mt. Kilimanjaro, respectively, and ends at the flanks of Lelatema mountain ranges in the south of the study area. The SAP covers parts of Kilimanjaro, Arusha, and Manyara regions. In the Kilimanjaro region, it covers parts of Siha district in the upper section whereas the central and southern section of the plain lies within Hai district. In Arusha, the plain covers parts of Meru and Arusha districts in the south-east flanks of Mt. Meru whereas, in Manyara, it covers the northern part of the Simanjiro district. In total, the SAP covers parts of 75 wards (~8550 km^2) with a total population of approximately 1 million (NBS, 2018). Some parts of the SAP are densely populated with settlements spatially distributed in the elevated terrain and along the major rivers, that is, Sanya and Kikuletwa that originate from Mt. Kilimanjaro and Mt. Meru, respectively.

The presence of fertile volcanic soils and easy access to groundwater resources SAP has attracted intensive irrigated agriculture within the SAP. The staple food crops grown include maize, beans, and vegetables such as onions, cabbages, tomatoes, spinach, carrot, etc. The SAP further supports nomadic

pastoralism, especially among Maasai communities in the central and southern parts of Hai, Meru and Simanjiro districts. Due to relatively extreme aridity and the absence of surface water in the SAP, both urban and rural communities depend on groundwater as a primary source of water for various purposes including drinking. Usually, groundwater is accessed through hand-dug wells, machine dug shallow wells, boreholes, and springs.

In terms of land cover, the SAP is dominated by the scrub, scattered trees and woodland in some parts of its extent. The parts in the northeast and northwest, especially near the flanks of the major stratovolcanoes (Mt. Kilimanjaro and Mt. Meru), are dominated by woodland, some of which are within the national parks. Most of the northern parts are dominated by the scattered trees while the central and southern parts are dominated by scrubland. Due to the availability of surface water from rivers near the flanks of the major stratovolcanoes, the north-eastern and north-western parts of the plain are extensively used for agriculture in terms of plantation. Similarly, the availability of perennial rivers and the development of shallow aquifers within the SAP, especially along the active Kikuletwa and Sanya river floodplains have attracted intensive irrigated agriculture.

The climatic condition of the SAP is controlled by the present geological setting and topographical landforms. The central part of the plain is the relatively driest section due to its flat low-lying ground between the two major stratovolcanoes in the northeast and northwest as well as the Lelatema mountains in the south (Fig.1). The presence of highlands in the north and south of the plain results in a highly variable climatic condition in terms of rainfall and temperature.

[Insert Figure 1]

1.1.2 Topography and groundwater flow conceptualization

The overall elevation of the study area lies between 650 and 5885 meters (Fig. 2). The SAP lies between 650 and 1600 meters while elevation between 1600 and 5885 meters is dominated by relatively

steep slopes of the stratovolcanoes. The major stratovolcanoes including Mt. Kilimanjaro, Mt. Meru, and the Lelatema mountains are primary recharge areas of the volcanic aquifers.

Two major groundwater flow paths are present in the study area. In the first case, groundwater flows to the north (Ghiglieri et al., 2010) while the second one is characterized by groundwater flowing to the south as reflected by the the overall major river flow directions in Figure 2. In the first case, aquifers discharge their waters in the major rift valley lakes (Lake Manyara and Lake Natron at the foot of the western EARV escarpment (Fig.1). Major rivers in this flow include Engare Nairobi (South), Engare Nairobi (North), and Engare Rongoi that drain Mt. Kilimanjaro in the northeast of the plain while the other river is Ngare Nanyuki which drains Mt. Meru in the north-west. The south flow is characterized by aquifers discharging their waters in the Pangani river, which eventually discharges its water in the Indian Ocean in the southeast. Major rivers in this flow direction include Kikuletwa and Sanya , which drain Mt. Meru and Kilimanjaro, respectively. The SAP considered in this study overlies aquifers discharging their waters in the Pangani river. Two aquifer types exist in the SAP including unconfined and confined aquifers with varying yield estimates (Ghiglieri et al., 2010). The unconfined aquifers are shallow with a depth to groundwater ranging between 1 and 5 m below ground level while for confined aquifers it ranges between 6 and 30 m below ground level. According to the completed well drilling and unpublished reports, the estimated yield for all aquifers ranges between 50,000 and 175,000 liters per hour (l/hr).

[Insert Figure 2]

2. Materials and methods

2.1 Spatial data compilation and preparation

Spatial data used in this study were collected from four sources including completed borehole drilling reports, open-access archives, existing national GIS datasets, and field surveys. The description of the specific spatial data types and sources are summarized in Table 1.

[Insert Table 1]

2.1.1 Field data collection

The field data collection involved water sampling from 14 boreholes and 9 springs along the SAP. The water sampling was done at two epochs. The first epoch was at the end of the short dry season in March 2018 while the other was at the end of the long dry season in December 2020. During the second epoch, water samples were collected from 4 boreholes since the rest of theboreholes were malfunctioning due to pump failure and electricity problems (personal communication with the Chairperson of the Sanya Plain Irrigation Scheme during fieldwork, December 2020). Furthermore, water samples from springs along the Sanya river channel were collected during the second epoch. The surface elevation at each borehole and spring was determined during epoch two by Global Navigation Satellite Systems in Real-Time Kinematic (GNSS RTK) method using two GNSS receivers (Hi Target V90).

The survey was conducted in two stages, where in stage one, the elevations for all study boreholes and springs were determined. The surface elevation (H) for each study location was determined by differential leveling using equation 1:

$$H = H_0 - (hi + ht) \quad (1)$$

where H_0 is the orthometric height at the base station, hi is the height of the instrument at the base station and ht is the height of target at rover station. The last two parameters were measured in situ using a 1 mm level steel tape measure at every set up during the field survey work while the first was obtained from the SMD (Table 1).

In stage two, F^- concentration in groundwater was measured in situ at each study location. Groundwater samples were collected according to the standard operating procedures for water sampling (WHO, 2017), where a 1-liter clean plastic (polyethylene) bottle was used for water sampling. The sampling bottles were rinsed three times with distilled water before collecting the water sample. The measurement of F^- was carried out immediately at the sampling point using an Ion-Selective Electrode, in

accordance with the standard analytical methods (APHA, 1989; WHO, 2017; HACH, 2021). Fluoride Ion Meter (HQ440D) was calibrated using the standard fluoride solutions supplied by Hach. In a typical procedure, 25 mL of water sample was mixed with 1 pillow of fluoride total ionic strength adjustor buffer (TISAB) powder in a beaker and shaken thoroughly to ensure that the TISAB powder is completely dissolved and uniformly mixed with the water sample to be analyzed. The same procedures were used for calibration and sample testing.

2.3 Geostatistical analysis

Since F^- in groundwater around Meru stratovolcano is highly variable in space, characterised by the large range in concentration (Bennett et al., 2021; Ghiglieri et al.,2010; Ijumulana et al., 2020), geostatistical analysis methods were used to study the spatial distribution of F^- concentration and their variation in space along selected sections within the SAP. The study was done in two stages, including spatial distribution assessment of F^- concentration around major stratovolcanoes surrounding the SAP in stage one and monitoring the effects of spatial variability of the geogenic sources on the F^- distribution within the SAP in stage two.

2.3.1 Spatial distribution analysis

Since water quality parameters were determined at the existing irregularly spaced and clustered groundwater sources, the ordinary kriging (OK) spatial interpolation method was used to systemize the sampling locations. The OK is one of the geostatistical methods commonly used for characterizing spatial variability and interpolating between sampled points (Yasrebi et al., 2009). It is used to account for spatial dependence in the observed events where the expectation is unknown creating immense complexities which cannot fully be accounted for by classical statistical models (Chiles and Delfiner, 2009). For this study, F^- concentration was spatially interpolated at 0.5 by 0.5-kilometer grid, which was the minimum separation distance between two nearest pairs of groundwater sampling locations. The validation of the interpolation map was done using field resampling at selected groundwater sources.

2.3.2 Analysis of the effects of terrain slopes on fluoride distribution in the Sanya alluvial plain

The effects of the variability of terrain slopes on the spatial distribution of F^- concentration in the SAP was studied at three sections. The first and third sections were cross-sectional studies along the groundwater divide in the north where the SAP starts (Sanya Juu) and along Kikuletwa river where the SAP ends (Sanya Chini), respectively. Section A-B comprised the two major stratovolcanoes, Mt. Meru in the west and Mt. Kilimanjaro in the east. The selection of this section was guided by the orientation of the debris avalanches due to the collapse of the eastern side of the Meru stratovolcano (Delcamp et al., 2017). The second section was a longitudinal profile along the Sanya river valley. The three study sections are represented in Figure 3 as sections A-B, C-D, and E-F for sections 1, 2, and 3, respectively. The elevation in the study sections varied between 900 and 3285 m, 800-1650 m, and 680-1100 m for sections 1, 2, and 3, respectively. The selection of these sections was based on the recently published work by Ijumulana et al. (2020) and was part of the identified regional fluoride contamination hotspot in groundwater sources. In all sections, the study span was 10 kilometers selected based on the spatial distribution of drinking water sources in the national fluoride database (Water Quality Service Division, 2016; Ijumulana et al., 2020). Furthermore, the distribution of F^- concentration along each section was interpreted based on the generalized terrain slopes calculated as:

$$m = \frac{\Delta \mathrm{H}_i}{d_i}, \tag{2}$$

with

$$\Delta \mathrm{H}_i = H_u - \mathrm{H}_l \tag{3}$$

and

$$d_i = \sqrt{(\mathrm{E}_u - \mathrm{E}_l)^2 + (N_u - N_l)^2} \tag{4}$$

where, m is the terrain slope between two consecutive contour intervals at an interval of 20 m, which is the national mapping standard contour interval in Tanzania, ΔH_i is the difference in elevation between the upper (H_u) and lower (H_l) contours at section i; d_i is a horizontal equivalent, which is the distance between two consecutive contours, $(E, N)_u$ and $(E, N)_l$ represent easting (E) and northing (N), respectively

defining the position of a point at the location *i* along the study section. During the terrain slope estimation, the constant variation at an interval of 20 m in elevation was assumed and the contours were generated from a 30 m resolution GDEM (Table 1) using the contour function in the spatial analyst toolbox of ArcGIS 10.6.1 software.

During the analysis, exploratory spatial data analysis (ESDA) tools were used. The ESDA tools contain graphical and analytical methods to visualize relationships between multiple variables (Haining et al, 1998; Symanzik, 2014). The spatial variation in F^- concentration was interpreted graphically based on the distances (chainages) and the generalized terrain slopes along each study section.

[Insert Figure 3]

2.2 Analysis of the effects of spatial variability of other geogenic sources on the distribution of fluoride concentration in the Sanya alluvial plain

The other geogenic sources studied in this research were depth to groundwater (depth to water table), borehole depth, screening depth, and irrigated agricultural practices in the SAP. The selection of the SAP was based on the data availability and its economic importance in terms of intensive irrigated agricultural practices which solely depend on groundwater as a primary source for irrigation. Both ESDA and regression analysis using ordinary least squares (OLS) estimation methods were used to explore the association between the distribution of F^- concentration and the spatial variability of depth to groundwater, borehole depth, screening depth, groundwater level, and surface elevation. The effects of depth on groundwater, borehole depth, and screening depth to the spatial distribution of F^- concentration were studied at 11 borehole locations while that of groundwater level and irrigation practices were studied at 9 springs along the Sanya river channel.

2.3 Regression analysis

The regression analysis by OLS estimation method is a classical method widely used to explore the relationship between two or more variables in which one is a response or dependent variable while others are explanatory or independent variables. The working principle of the method is based on standard regularity conditions (Anselin, 2001). The selection of this (OLS) was based on exploratory spatial data analysis (Haining et al., 1998), which indicated an absence of significant violation of standard regularity conditions in the observed F^- concentration. The OLS regression model used is represented in equation 5 (Hoch, 2012):

$$Y_i = \beta_0 + \beta_1 X_i + \varepsilon_i \quad (5)$$

where Y_i is an *n x 1* vector of observations on the dependent variable (F^- concentration), β_0 is a regression constant, β_1 is a *k x 1* vector of coefficients representing the relationship between response and predictor variable *X (*depth to groundwater, borehole depth, screening depth, groundwater level, and surface elevation), X_i is an *n x k* matrix whose elements are observations on predictor/explanatory variable, and ε_i is an *n x 1* vector of errors at every observation *i*.

The data on depth to groundwater, borehole depth, and screening depth were obtained from drilling borehole reports while that on surface elevation were estimated using equation 1. Groundwater level was calculated as:

$$GWL = H - SWL \quad (6)$$

$$SD = 3n \quad (7)$$

where H is surface elevation and SWL is the depth to groundwater obtained directly from the drilling borehole reports in Table A1. The constant 3 in equation 7 is the screening interval while n is the total number of screens counted arithmetically from the borehole logs.

2.3.1 OLS regression model fit

The model fit was evaluated at two scenarios. In the first scenario, the overall model fit was evaluated using calculated adjusted R^2 and the F-test statistic at a 0.05 significance level. In the second scenario, the significance of individual coefficients $\widehat{\beta_1}$ was evaluated using a t-statistical test at 0.05 significance level.

2.3.2 OLS regression model robustness

The model robustness was evaluated based on the model diagnostics. These included spatial and non-spatial diagnostics. The non-spatial diagnostics included assessing the presence of multicollinearity problem in F^- concentration and among the explanatory variables, test on the normality of the regression residuals (ε_i), and test on the heteroskedasticity (constant error variance). For the multicollinearity problem, the multicollinearity condition number was calculated and used to infer the dependence between observed values on F^- concentration and among the explanatory variables. As a rule of thumb, the non-existence of multicollinearity problem is when the calculated number lies within or below the range of 30 and 50 (Belsley, et al., 2005). The statistical test on the normality in the error terms was done using the Jarque-Bera test (Jarque and Bera, 1980) while the heteroskedasticity problem was assessed using the Breusch-Pagan test (Breusch and Pagan, 1979). In addition, the robustified version of the latter test, i.e, the Koenker-Bassett test (Koenker and Bassett, 1982) was used. All the statistical tests were done at a 0.05 significance level. The spatial diagnostics included testing the presence of spatial autocorrelation in the regression residuals. The Moran's I statistic was used in this regard (Moran, 1950). Likewise, this test was done at a 0.05 significance level.

2.5 Software used in this study

The GIS, statistical and spatial statistical software were used in this study. The GIS software included ESRI ArcGIS 10.6.1 and QGIS 2.18.23. These software were used for spatial data compilation, preparation, and mapping purpose. The statistical software used was RStudio 1.2.5042. The software was used for classical exploratory analysis and visualization of some results in this study. The spatial statistical software used was GeoDa 1.14.0. It was used for spatial analysis of F^- concentration in space.

3. Results and discussion

3.1 The statistical and spatial distribution of fluoride concentration around the Sanya plain

The statistical distribution of F^- concentration generated from 517 groundwater sources with 0.08, 0.64, 2.10, 6.57, and 74.00 mg/L as a minimum, 1st, 2nd, and 3rd quartiles, and maximum value, respectively is presented in Figure 4a. The interquartile range (IQR), mean, and standard deviation (s.d) were estimated as 5.93, 5.49, and 8.44 mg/L, respectively.

According to Dissanayake (1991) health risk classification system, 22.1 (114), 20.3 (105), 19.5 (101), 21.9 (113) and 16.2 (84)% of groundwater sources had F^- concentration <0.5, 0.5-1.5, 1.5-4.0, 4.0-10.0 and > 10.0 mg/L, respectively. Approximately 97% of groundwater sources with F^- concentration <0.5 mg/L were spatially distributed around the flanks of Mt. Kilimanjaro where approximately 1 million people are at high dental caries risk (Ijumulana et al., 2021). Other groundwater sources in this category were distributed in the southern flanks of Mt. Meru.

For groundwater sources with F^- concentration between 0.5 and 1.5 mg/L, the safe range (WHO, 2011; 2017), approximately 84% were spatially distributed in the south flanks of Mt. Meru while 11% and the rest were distributed in the south-western flanks of Mt. Kilimanjaro and within the SAP, respectively (Fig.4a). The high frequency of safe drinking water sources in the southern flanks of Mt. Meru correlates with the high density of volcanic domes (Fig.4b) suggesting that the spatial variability of F^- concentration in this setting may be caused by the mixing of water with high concentration from the primary recharge area, the Arusha National Park, and that from secondary recharge areas, which are the volcanic domes. This is also the case for groundwater sources in the south-western flanks of Mt. Kilimanjaro. For groundwater sources in the SAP, most of them were shallow wells and appeared at relatively steeper slopes in the upper section while others were located within the Kikuletwa flood plain whose water is a mixture of recharge water from Mt. Meru in the north and Lelatema mountains in the south.

Groundwater sources with F^- concentration > 1.5 mg/L (57.6%) were spatially distributed around the flanks of Mt. Meru and those with higher concentration (above 10.0 mg/L) dominated the lower slopes of Mt.Meru and the central part of the SAP. Places with higher concentration consisted of fewer or no stratovolcanoes which provide secondary recharge to aquifers in the alluvial plains in the low lands of major stratovolcanoes. Thus, there is no natural dilution of the primary recharge water, and due to the longer contact time between water and fluoride-bearing rocks, the dissolution processes result in the release of fluoride ions into groundwater. On the other hand, many groundwater sources with extreme F^- concentration were distributed in the leeward side, west of Mt. Kilimanjaro, which is part of the semi-arid northern Tanzania (Solomon et al., 2000) that receives little annual rainfall suggesting that inadequate recharge of aquifers in these settings resulting into high F^- concentration.

The spatial distribution of F^- concentration around the SAP is presented in Figure 4b. The F^- concentration varied in space with the highest concentration forming patterns in the northern, and all over the south-eastern parts of Mt. Meru. In these parts, the predicted F^- concentration ranged between 5 and 20 mg/L with the highest values between 10 and 20 mg/L clustered within the SAP. The shape formed by the highest predicted F^- values correlated with the structure of the debris avalanche deposits formed by the collapsed eastern side of Mt. Meru. The collapse of Mt. Meru is amongst the largest debris avalanches in the world with deposits reaching the foothills of Mt. Kilimanjaro (Wilkinson et al., 1986; Delcamp et al, 2017, Kisaka et al., 2021). The north to the south-east extent of the spatial pattern formed by the predicted highest F^- values along the SAP suggests that the spatial variability of F^- is highly controlled by the presence and water interactions with debris-avalanche deposits rich in fluorine-bearing mineral phases such as titanites, amphiboles, hornblende and pyroxenes (Ijumulana et al., 2020; Kisaka et al., 2021).

The predicted lowest concentration existed around Mt. Kilimanjaro and formed a northwest to southeast stretch. Similarly, the lowest F^- concentration were found around Arusha city located at the the south flanks of Mt. Meru (Fig. 4b). The predicted F^- concentration in this zone ranged between 0.10 and 2.50 mg/L. Places with F^- concentration above 1.5 mg/L around the flanks of the major stratovolcanoes

may be related to the mixing of water with low and high concentration originating from aquifers in the primary recharge areas (Kilimanjaro and Arusha National Parks) and those in the SAP, respectively. Similarly, the presence of low concentration in the neighborhood of high concentration, particularly in the southern flanks of Mt. Meru dominated by minor stratovolcanoes, can be explained as the mixing water originating from the primary recharge area (Arusha National Park) and that from secondary recharge areas around the minor stratovolcanoes (Fig.4b). In comparison, the largest extent of the zone with the highest predicted F^- concentration existed within the central part of the SAP presenting a high-risk level to the communities which solely depend on groundwater for various purposes in general and drinking in particular within the Pangani drainage basin (Ijumulana et al., 2021). The presence of elevated F^- concentration within the central part of the plain can be explained in two incidences. In the first incidence, the plain consists of few or no minor stratovolcanoes which act as secondary recharge areas in the flanks of the major stratovolcanoes leading to little or no natural dilution of groundwater from the latter aquifers. In the second incidence, secondary mobilization of F^- is possible through the dynamics of the debris avalanche deposits dominated by volcanic ashes (Kisaka et al., 2021), which are naturally rich in fluoride content (Brindha and Elango, 2011). Wind and surface water run-off erosion and deposition processes during dry and wet seasons, respectively cause dynamics of the debris avalanche deposits, creating a large scale of variation in F^- in the lowlands of the SAP (Fig.4a). Other causes to the dynamics of the debris avalanche deposits include human activities, especially irrigated agriculture and nomadic pastoralism within the plain. These activitiescould be affecting the physical charecteristics of the deposits, thus accerelating their erosion and deposition processes leading to the widespread flushing of F^- in the groundwater of the SAP, especially at the shallow depths. In addition, the larger vadose materials thickness made of the debris avalanche deposits could be enhancing the contact time between groundwater and fluoride-bearing volcanic rocks/soils/sediments during the recharge periods. This phenomenon is considered as among the secondary causes of the high spatial variability of F^- concentration in groundwater(Ghiglieri et al., 2010; Ali et al., 2021).

[Insert Figure 4]

3.2 Spatial variability of terrain slopes and distribution of fluoride concentration in the Sanya alluvial plain

The spatial variability of the generalized terrain slopes and spatial distribution F^- concentration along the three sections is summarized in Figure 5a-c. In each section the predicted F^- concentration are indicated at the left, central and right sections (detailed in section 2.3.2). In addition, the raw data within 10-kilometer coverage along each profile are represented as blue dots in each section.

In terms of raw data, F^- concentration varied between 0.16-32.00, 0.20-75.00, and 0.80-63.00 mg/L along the groundwater divide, where the SAP starts (Fig.5a-1), along Sanya river valley (Fig. 5c-1) and across Sanya floodplain, along Kikuletwa river where the SAP ends (Fig. 5b-1), respectively. Both the minimum and maximum concentration values in the Sanya river valley and across the floodplain were greater than those along the groundwater divide. Considering the minimum and maximum values in all sections, a trend of increasing concentration of F^- is observed downstream which is related to the increased contact time between groundwater and fluoride-bearing aquifers sediments predominantly comprising volcanic soils and sediments. The groundwater-and its interaction with the aquifer sediments is therefore an important factor triggering the high variability of F^- concentration in groundwater systems within the SAP (Ghiglieri et al., 2010). The highest F^- concentration along the groundwater divide appeared close to the collapsed side of Mt. Meru which is dominated by the vitric andosols, the volcanic soils that develop on top of volcanic ashes which are well-known sources of elevated F^- concentration in the environment (Cronin et al., 2003; Brindha and Elango, 2011; Vithanage and Bhattacharya, 2015).

In terms of predicted F^- concentration, the predicted minimum, and maximum values indicated increasing trends along the three sections. The minimum increased from 0.16, 1.00 to 2.22 mg/L and 0.15, 2.79 to 3.06 mg/L for the left and central profile of Figure 5(a-1,b-1 and c-1), respectively. No observed

trend in the variation of the predicted minimum value for the right profile. However, the highest value (7.93 mg/L) was observed along the Sanya river valley (Fig. 5b). Comparing the predictions in the upstream of the Sanya plain along the groundwater divide and downstream across the Sanya floodplain, the minimum increased from 0.13 to 2.26 mg/L, respectively. For the predicted maximum value, no trend was observed for the left profile although it increased from 13.15 to 17.69 mg/L along the groundwater divide and across the Sanya floodplain, respectively (Fig. 5(a-1 and c-1)). The predicted maximum value was 8.52 mg/L along the Sanya river valley (Fig. 5b-1). The predicted low value in the maximum along this profile could be the result of high spatial variability and few raw data points in the upper and central section of the Sanya plain.

In comparison with the maximum recommended value of 1.5 mg/L for drinking water (WHO, 2011), few samples in all sections had less than 1.5 mg/L as represented by the red line in Fig. 5. In Fig. 5a-1, groundwater sources with F^- concentration less than 1.5 mg/L existed in the southeast flanks of Mt. Kilimanjaro at an elevation between 1000 and 1500 meters. Groundwater sources with F^- concentration close to 1.5 mg/L existed around the southern flanks of Mt. Meru while others were in the southwest flanks of Mt. Kilimanjaro. The groundwater sources with slightly high F^- concentration existed close to the eastern boundary of the Sanya plain. In Fig. 5b-1, three groundwater sources had F^- concentration below 1.5 mg/L and existed at an elevation between 800 and 850 meters within volcanic valleys at the south-western flanks of Mt. Kilimanjaro upstream of the Sanya plain. This is in line with the predicted F^- concentration in left profile which is relatively flat indicating potential sources for safe drinking water. On the other hand, the highest F^- concentration with a large scale of variation downstream, which is dominated by the Sanya floodplain, was observed. The presence of high values of F^- concentration in the Sanya floodplain can be associated with the high rate of debris avalanches deposition (Fig.4a) determined by the flat sloping terrain that enhances the contact time between groundwater and fluoride-bearing volcanic rocks and soils during the recharge period and groundwater flow process.

In Figure 5c-1, most groundwater sources are concentrated in the Sanya floodplain. However, few of them are of acceptable quality for drinking purposes and existed in the western part of the floodplain at an elevation between 600 and 620 meters. The spatial variability in F^- concentration may be originating from the mixing of surface water along the Kikuletwa river and aquifers with a primary recharge in Mt. Meru and other minor stratovolcanoes in the south flanks of Mt. Meru (Fig.4b). The largest variation was observed at the Kikuletwa and Sanya river confluence.

[Insert Figure 5]

In terms of terrain slopes along the three sections, predicted F^- concentration were inversely proportional to the generalized terrain slopes. While the terrain slopes varied between -15 and 117% with an average slope of 11±29% along the groundwater divide (Fig.5a-2), they ranged between -2 and 15%, and between -0.03 and 4% along the Sanya river valley and Kikuletwa river, respectively. Average slopes along the three sections were 11±29%, 0±1%, and 0±1% along the groundwater divide, Sanya river valley, and Kikuletwa river, respectively. Along the three sections, F^- concentration increased with distance from highlands (relatively steep slopes) and demonstrated the high spatial variability in the central SAP.

Furthermore, an increasing trend in F^- concentration along the groundwater divide up to 5 kilometers at an elevation of ~1600 meters, which defines the foot of Mt. Meru and the beginning of the SAP (Fig.5a-2) was observed. Despite no trend was visible between 5 and 15 kilometers along the same section, the spatial variability was high and correlated with the variability in terrain slopes, which may suggest the mixing of recharge water from minor stratovolcanoes along the groundwater divide with that from Mt. Meru aquifers. The section between 15 and 23 kilometers was approximately flat and F^- concentration increased explaining the effect of contact time between the debris avalanche deposits and

groundwater. A decreasing trend in F^- concentration beyond the 23-kilometer section, dominated by the Sanya river valley and the foot of Mt. Kilimanjaro at an elevation of ~1380 meters, is an indication of the natural dilution through the mixing of high and low F^- water from Mt. Meru and Mt. Kilimanjaro aquifers, respectively.

Similarly, an increasing trend in F^- concentration along the Sanya and Kikuletwa river valleys up to 20 and 29 km, respectively (Fig.5b-2 and c-2) was observed. In both sections, there was a general decrease in terrain slope although the rate of change was relatively lower along the Kikuletwa river valley (Fig.5c-2) compared to that of the Sanya river valley (Fig.5b-2). For the section between 20 and 33 km along the Sanya river valley, no trend was observed despite F^- concentration indicated multivariate variation. Part of this section is dominated by the Sanya floodplain, which starts at around 1000 meters elevation and is dominated by irrigated agriculture. The multivariate nature of F^- concentration in the Sanya flood plain can be associated with the mixing of shallow and deep water, especially during the dry season when the latter with high content of F^- mixes with the former having less F^- concentration. The section beyond 33 km of Figure 5b-2 was characterized by a decreasing trend in F^- concentration where the lowest concentration were close to the Kikuletwa river channel. The presence of relatively low F^- concentration may be due to the mixing of water from aquifers in the Lelatema mountains (LM) and that from shallow aquifers in the Kikuletwa river valley. The large scale of variation in F^- concentration between 20 and 30 km section along the Kikuletwa river valley (Fig.5c-2) can be associated with irrigated agricultural activities within the Sanya floodplain. The decreasing trend in F^- concentration beyond 30 km along the Kikuletwa river valley can be explained by the mixing of low F^- water from Mt. Kilimanjaro aquifers and high fluoridated water from Mt. Meru aquifers.

3.3 Spatial variability of the sources and distribution of F^- concentration in the Sanya flood plain

Table A2 presents the data used to study the spatial variation of the sources and distribution of F^- concentration in the Sanya floodplain Although it was not one of the objectives of this study, several

boreholes were not operational till 2020 due to malfunctioning of water pumps and electricity problems leading to missing groundwater samples during the second sampling campaign in December 2020. Likewise, springs along the Sanya river channel were not sampled during the first epoch in March 2018 due to inaccessibility problems. In Table A2, *n.d* and *n.m* stand for value not determined and not measured, respectively.

3.3.1 Spatial variability of depth to groundwater and distribution of fluoride concentration

Figure 6 shows ESDA results for F^- concentration in groundwater and variability in depth to groundwater.concentration. At the springs, F^- concentration varied between 4.00 and 7.00 mg/L, exclusive while they varied between 4.00 and 32.00 mg/L, exclusive in boreholes (Fig.6a-1). In other words, all groundwater sources were not suitable for drinking purposes (WHO, 2011). Fluoride concentration in the boreholes demonstrated the highest scale of variation as represented by the large interquartile range. In both cases, the highest F^- concentration values were located upstream of the Sanya river channel. The relatively low F^- concentration downstream are possibly due to the natural dilution from the mixing process of groundwater water from aquifers in the Lelatema mountains, south of the floodplain, and that from the south flanks of Mt. Kilimanjaro as also indicated by the relatively flat right profile in Figure 5c-1. Alternatively, the relatively low F^- concentration in the springs may be an indication of the presence of perched shallow aquifers developed in the fluvial deposits, with a limited spatial extent (Ghiglieri et al., 2010), discharging their waters in the Sanya river channel. Most of these springs dry up during the hot and dry season where the agricultural activities in the Sanya floodplain are supported by the highly F^- contaminated water from the drilled boreholes close to the irrigation furrow.

Figure 6a-2 shows the distribution of F^- concentration with depth to groundwater according to MacDonald et al. (2012) classification scheme. Two boreholes (~18%) were in the very shallow (<7 m) category while eight (~73%) were in the shallow (7-25 m) category. One borehole (~9%) was in the shallow to medium (25-50 m) category. None of the borehole locations existed in the medium (50-100 m), deep (100-250 m), and very deep (>250 m) categories. In both categories, the aquifer yield was

approximately equal to 20 l/s, which corresponds to the high aquifer productivity in the aquifer productivity classification system by MacDonald et al. (2012). The presence of multiple categories of depth to groundwater is a typical characteristic of complex hydrogeological environments in volcanic areas. Ghiglieri et al. (2010) in their study to locate a safe groundwater source in Ngarenanyuki and Oldonyosambu wards, in the north of Mt. Meru, identified four hydrogeological complexes that occurred within different volcanic formations, either alone or superimposed upon one another. They further reported that no aquifer was determined at a depth of 300 m while the depth to groundwater was shallow and shallow to medium at one and three locations, respectively.

Although the shallow to medium category had one sample, F^- concentration increased significantly with depth to groundwater and ~95% (adjusted R^2=0.95, $p < 0.05$) of the variation in F^- concentration was explained by a linear increase in depth to groundwater level. This implies that the spatial variability in the type of vadose materials, contact time between them and recharge water, permeability, and porosity of the unsaturated subsurface materials contribute significantly to the occurrence and spatial distribution in F^- concentration. Figure.8b shows the spatial variability of unsaturated subsurface materials as summarized from the national borehole drilling reports.

For the boreholes in the very shallow category, the dominating unsaturated subsurface materials included fine sand, fine to medium sand, silt, and gravel whose permeability is relatively high resulting in less contact time during the recharge period. For this reason, very shallow aquifers contain relatively low F^- concentration. However, this will depend on the type of the parent materials from which the materials were derived and the hydraulic gradient in the area of interest. In the shallow category, the unsaturated subsurface materials were dominated by both consolidated and unconsolidated sediments of volcanic origin. The unconsolidated sediments were clay, silt, sand, gravel, and pebbles whereas the consolidated materials included pyroclastics and basalts.

For the shallow to medium category, the unsaturated subsurface materials were dominated by fine to coarse sand and gravel with relatively enhanced permeability compared to the nearby borehole (BH548 at

1+760 m chainage) in the upstream which was dominated by fine to medium and fine to coarse sand with high F^- concentration. In general terms, F^- concentration varied in space with depth to groundwater as suggested by Figure 6b. It decreased significantly with a decrease in depth to groundwater, especially in the Neogene-Quaternary volcanic formations dominated by pyroclastics with alkaline volcanic lavas (Between BH548 and BH556). In contrast, F^- concentration increased downstream within the Mozambique belt (between BH556 and BH522) despite no significant change in depth to groundwater was observed. The relatively low concentration at BH510 may be due to less dominance in unconsolidated materials compared to the rest of the borehole locations. Furthermore, a slight increase in F^- concentration was observed between chainage 33+400 and 37+900 (Fig.6b). The boreholes in this section were located along the Kikuletwa river (Fig.7a). The increase in F^- concentration upstream of the Kikuletwa river corresponded with an increase in depth to groundwater. The upstream of the river is dominated by volcanic gravel and pebbles that have been transported from the highlands of Mt. Meru and deposited within the flooding plain of the river.

[Insert Figure 6]

3.3.2 Spatial variability of borehole depth, screen depth, and the distribution of fluoride concentration

Figure 7a shows the spatial variability of borehole depth and the distribution of F^- concentration. Generally, F^- concentration decreased with depth suggesting low concentration in the deeper aquifer. The largest change rate was observed in the Neogene-Quaternary volcanic formations dominated by pyroclastics with alkaline volcanic lavas (vpN-Q) section where F^- concentration decreased from 22.5 to 4.29 mg/L at a distance of around 7 kilometers from .borehole number. BH548. In contrast, F^- concentration increased with a decrease in depth from 4.29 to 12.5 mg/L at BH556 and BH522, respectively within a separation distance of ~4 kilometers within the Mozambique belt dominated by

Migmatite - granite - meta-sediment (marble, quartzite) complex (miNP). Similarly, a negative correlation between F^- concentration and depth was observed between BH524 and BH537 where F^- concentration increased from 4.51 to 7.60 mg/L at a separation distance of ~4.5 kilometers.

The large scale of variation between BH548 and BH556 correlated with the percentage of dominance by unconsolidated sediments within the screening depth (Fig.7b). The percentage of dominance was 53, 64, 49, and 23 at BH548, BH553, BH165, and BH556, respectively. Therefore, this suggests that unconsolidated sediments, particularly volcanic sediments comprising of fluoride-bearing fine, medium, and coarse sand together with gravel, clay, silt, and boulders contribute significantly to the spatial variability in F^- concentration within the Neogene-Quaternary volcanic formations. For the case of boreholes in the Mozambique belt, along the Sanya river valley (BH510, BH518, BH511, and BH522) in Figure 7a, an increase in F^- concentration correlated negatively with depth suggesting that shallow aquifers contain highly contaminated water unsafe for drinking purpose in this setting. The large scale of variation in the shallow aquifers also correlated positively with the percentage of dominance by the volcanic deposits suggesting that elevated concentration of F^- is mobilized from the tertiary-quaternary unconsolidated sediments, derived from the debris avalanche deposits dominating the eastern flanks of Mt. Meru (Ghiglieri et al., 2010; Kisaka et al., 2021). For boreholes along the Kikuletwa river valley (i.e, BH524, BH526, and BH537), the presence of relatively low F^- concentration at BH524 and high at BH526 and BH537 suggests that F^- is mobilized from volcanic deposits that are continuously transported and deposited within the river valley. The percentage of dominance for unconsolidated sediments was 100 and 67% at BH526 and BH537, respectively while it was 30% at BH524. The latter borehole was located outside while the former two were near within the river valley under intensive irrigated agriculture.

[Insert Figure 7]

In addition, Table 2 shows summary of regression analysis using OLS estimation method used to explain the relationships between depth to groundwater, borehole depth, and screen depth. Overall, approximately 78% (Adjusted R^2 =0.782) of the variation in observed F^- concentration was explained by a significant model at a significant level of 0.05 (F-statistic=11.730, p-value=0.006). At individual variables, a significant positive correlation between F^- concentration and depth to groundwater were observed as indicated by a large t-Statistic and p-value <0.05. Although not significant, a positive relationship between F^- concentration and screen depth was observed. In contrast, a significant negative correlation between F^- concentration and borehole depth was observed as evidenced by a large t-Statistic and p-value <0.05. Furthermore, Table 3 presents the OLS regression diagnostics mainly the test for normality in the regression residuals and test for heteroskedasticity using Jarque-Bera test (Jarque, and Bera, 1980), and Breusch-Pagan/ Koenker-Bassett tests (Breusch and Pagan, 1979; Koenker and Bassett, 1982), respectively. All the tests were not statistically significant at 0.05 significant level indicating that the regression errors/residuals were normally distributed and the error variance was constant. Likewise, there was no potential multicollinearity problem in the observations on the variables used in the model as indicated by the multicollinearity condition number <30 (20), which is a rule of thumb (Belsley et al., 2005)

[Insert Table 2]

[Insert Table 3]

The positive correlation between F^- concentration and depth to the water table is an indication that F^- could be mobilized from the vadose section overlying the aquifer. This was substantiated by most of the boreholes with high F^- concentration being clustered in the upstream of the Sanya river floodplain which is dominated by Vitric Andosols and pyroclastics with alkaline volcanic lavas. The depth to the water

table in this zone ranged between 14 and 24 m. An increased depth to the water table implies that recharge water from precipitation and any surface water body takes a longer time to reach the aquifer. The prolonged time may be an important factor in the mobilization of elevated F^- content in groundwater systems within the Sanya floodplain. The negative correlation between borehole depth and F^- concentration is an indication of the potential safe water in deep aquifers within the SAP. However, this is true for fractured basement aquifers where groundwater flow is high minimizing the contact time between groundwater and F^--bearing rocks.

3.3.3 Spatial variability of groundwater level and the effect of irrigated agriculture on the distribution of fluoride in groundwater

The effects of spatial variability of groundwater level and irrigated agricultural practices on the distribution of F^- concentration in groundwater are visualized on Figure 8. Fluoride concentration increased linearly with an increase in groundwater elevation at 0.05 significance level (Fig.8a) The occurrence of relatively high F^- concentration in the upper section of the flood plain, which is characterized by longer depth to groundwater, justifies that F^- is mobilized from the unsaturated subsurface materials during recharge periods from rainwater and irrigation water infiltration. The irrigation water from boreholes contains relatively high F^- concentration and this could be contaminating the perched aquifers existing in river valleys of the volcanic lowlands around the stratovolcanoes, which are primary recharge zones in volcanic regions of northern Tanzania (Ghiglieri et al., 2010). Furthermore, the high F^- concentration in the upper section of the flood plain can be associated with the existence of the Vitric Andosols, the volcanic soils developing on top of volcanic ashes, the debris avalanche deposits in this study, could be influencing the high concentration of F^- in groundwater. Naturally, volcanic soils contain high content of F^- (Brindha and Elango, 2011; Chowdhury et al., 2019). The deep soil profile, rapid hydraulic conductivity, and water holding capacity of most Andosols (Arnalds, 2015) are favorable conditions for the high rate of F^- mobilization in groundwater systems in volcanic regions of the world. Due to these conditions, the contact time between the Vitric Andosols, other unsaturated subsurface

materials (Fig.6b) and recharge water increases as recharge water percolates through them. Therefore, the longer depth to groundwater in the upstream increases the contact time between recharge water and fluoride-bearing volcanic materials thus enhancing dissolution processes of the fluoride-bearing mineral phases, particularly titanite, amphibole, hornblende, and biotite that are prevalent in the volcanic regions of northern Tanzania (Ijumulana et al., 2020).

In terms of lithological setting, the four intakes (NF, M*z*F, P*l*F, and CF) were in the pyroclastics with alkaline volcanic lavas (vpN-Q) while the rest (HF, M*g*F, PSF, KKF, and M*r*F) were located in the weathered/fractured Migmatite - granite - meta-sediment (marble, quartzite) complex (miNP). Intakes in the vpN-Q demonstrated relatively high F^- concentration suggesting the mobilization of F^- from weathering of fluorine-bearing alkaline volcanic rocks and dissolution of fluoride-bearing mineral phases within the pyroclastics and alkaline volcanic rock formations (Brindha and Elango, 2011; Vithanage and Bhattacharya, 2015). The relatively low fluoride concentration in the miNP setting may be due to the reduced contact time as most of the metamorphic rocks in the miNP complex are highly fractured leading to reduced contact time between recharge water and rocks probably due to high groundwater flow rate.

Figure 8b visualizes the possible effects of irrigated agricultural practices on the distribution of F^- concentration along the Ngomeni irrigation furrow (NF). Although not significant at 0.05 significance level, approximately 44% of the variation in the measured F^- concentration was explained by the OLS regression model. The insignificant model outcome might have resulted from a multicollinearity problem caused by the closeness of observed surface elevations (H), which is a typical topographic characteristic of the Sanya floodplain. At the intake (NF), F^- concentration varied between 6.22 and 6.29 mg/L while it increased to around 6.55 mg/L downstream. The difference in surface elevation at the intake and the last sample downstream along the furrow was 12 m at a separation distance of approximately 2 kilometers resulting in a slope of approximately 0.6%. Due to this relatively flat ground, F^- concentration could be mobilized from Vitric Andosols in the earthed irrigation furrows during farming practice as the contact time between groundwater and soils increases. In this regard, the irrigated agricultural practices using

highly F^- contaminated water from deep aquifers could be a potential source of high-scale variation in hand-dug wells and shallow wells within the Sanya flood plain.

[Insert Figure 8]

4. Conclusions

In this research, the spatial variability of the sources and distribution of F^- and the potential mechanisms of the mobilization of F^- in groundwater resources of the SAP were studied. Most of the groundwater sources with the highest F^- concentration above WHO recommended guideline for drinking water are concentrated in the central part of the SAP posing a high fluorosis risk to the population in this setting. The orientation of the main F^- pattern with high concentration above 8 mg/L in the upper section of the SAP correlates with that of the collapsed side of the Meru stratovolcano suggesting that the debris avalanche deposits are the primary sources of F^- in most of the tertiary-quaternary unconsolidated and volcanic aquifers. The favorable conditions, particularly the water holding capacity of vitric andosols in the SAP furthermore enhance the dissolution processes of F^- bearing minerals due to the increased contact time in the vadose zone of the local aquifers.

The distribution of F^- concentration in groundwater systems of the SAP was found to be controlled by spatial variability in terrain slope with potential safe groundwater sources close to the flanks of the stratovolcanoes.concentration. Despite depth to groundwater is of economical importance in groundwater access and supply, it has an impact on the quality of drinking water in the geogenically contaminated aquifers as it determines the contact time between unsaturated subsurface materials and recharge water.

The current practice to access groundwater in the SAP contributes to the exposure to F^- related hazards of the population. The deeper aquifers contain low F^- concentration and are characterized by weathered and fractured basalts, pyroclastics, and phyllites. Most of these aquifers likely experience

regional recharge from the volcanic highlands and are confined in nature. However, the decision on the screening depth during borehole development could be contributing to the contermination of the deep aquifer waters. Though not statistically significant, the boreholes where the screening depth was dominated by unconsolidated aquifer materials such assand, gravel, volcanic soils and pebbles, etc had relatively higher F^- concentration. The current irrigated agricultural practices using F^- contaminated water from the deep water table in the SAP contribute to the high spatial variability in F^- concentration in the perched shallow aquifers within the Sanya floodplain.

The findings of this study are important to the overall chain of safe water supply process in historically fluorotic regions of the world. In Tanzania, these findings can improve the current process of drilling permits issuance at the basin level. To the local drillers, the findings bridge the spatial uncertainty when deciding the location of the safe source, screen depth as well as depth to avoid targeting unsafe hydrogeological layers.

Acknowledgment

The authors extend their sincere thanks to Swedish International Development Cooperation Agency (Sida) for the funding through the FAHWAT project (Sida Contribution 51170072, Project No. 2235). Co-author Ines Tomašek acknowledges the support received from the Agence Nationale de la Recherche of the French government through the program "Investissements d'Avenir" (16-IDEX-0001 CAP 20–25). All government agencies who shared with us spatial data used in this study are deeply appreciated. Special appreciation goes to the Director of Water Quality Division of the Ministry of Water Resources of The Government of the United Republic of Tanzania for allowing us to access the National Fluoride Database and use F^- data to prepare this publication. Last but not least, authors do appreciate the Director-General of the Pangan Water Basin Office for providing us with core data based on completed borehole drilling reports.

Declaration of conflict of interest

No potential conflict of interest.

Credit Author Statement

Julian Ijumulana: Conceptualization, Methodology, Data analysis, Writing-original and final draft preparation **Fanuel Ligate:** Writing-Reviewing and Editing: **Regina Irunde:** Writing-Reviewing and Editing **Prosun Bhattacharya**: Conceptualization, methodology, Writing- Reviewing and Editing, Project administration. **Arslan Ahmad:** Writing-Reviewing and Editing. **Ines Tomašek:** Writing-Reviewing and Editing. **Jyoti Prakash Maity:** Writing-Reviewing and Editing. **Felix Mtalo***:* Supervision, Project administration.

References

Adelana, S. M., Macdonald, A. M., 2008. Groundwater research issues in Africa. *Applied groundwater studies in Africa. Taylor and Francis, London*, 1-8.

African Ministers' Council on Water (AMCOW), 2012. Status report on the application of integrated approaches to water resources management in Africa. *African Ministers' Council on Water*, Abuja, Nigeria.

Ali, S., Shekhar, S., Chandrasekhar, T., Yadav, A. K., Arora, N. K., Kashyap, C. A., Chandrasekharam,D., 2021. Influence of the water-sediment interaction on the major ions chemistry and fluoride pollution in groundwater of the Older Alluvial Plains of Delhi, India. *Journal of Earth System Science, 130*(2), 98. https://doi:10.1007/s12040-021-01585-3.

APHA, 1989. Standard Method for Examination of Water and Wastewater, 17th Ed. *American Public Health Association*. Washington DC, USA.

Anselin, L., 2013. Spatial econometrics: methods and models (Vol. 4): *Springer Science & Business Media*.

Anselin, L., 2001. Rao's score test in spatial econometrics. *Journal of statistical planning and inference, 97*(1), 113-139. https://doi.org/10.1016/S0378-3758(00)00349-9.

Arnalds, O., 2015. Andosols—Soils of Volcanic Regions. In *The Soils of Iceland* (pp. 47-54). Dordrecht: Springer Netherlands.

Belsley, D. A., Kuh, E., Welsch, R. E., 2005. Regression diagnostics: Identifying influential data and sources of collinearity (Vol. 571): *John Wiley & Sons*.

Bennett, G., Van Reybrouck, J., Shemsanga, C., Kisaka, M., Tomašek, I., Fontijn, K., Kervyn, M., Walraevens, K., 2021. Hydrochemical Characterisation of High-Fluoride Groundwater and Development of a Conceptual Groundwater Flow Model Using a Combined Hydrogeological and Hydrochemical Approach on an Active Volcano: Mount Meru, Northern Tanzania. *Water, 13*(16), 2159. https://www.mdpi.com/2073-4441/13/16/2159

Bhattacharya, P., Adhikari, S., Samal, A. C., Das, R., Dey, D., Deb, A., Ahmed, S., Hussein, J., De, A., Das, A., Joardar, M., Panigrahi, A. K., Roychowdhury, T., Santra, S. C., 2020. Health risk assessment of co-occurrence of toxic fluoride and arsenic in groundwater of Dharmanagar region, North Tripura (India). *Groundwater for Sustainable Development, 11*, 100430. https://doi.org/10.1016/j.gsd.2020.100430.

Braune, E., Xu, Y., 2008. Groundwater management issues in Southern Africa. An IWRM perspective, (IWRM Special Edition) *Water SA* 34(6).

Bretzler, A., Johnson, C. A., 2015. The Geogenic Contamination Handbook: Addressing arsenic and fluoride in drinking water. *Applied Geochemistry, 63*, 642-646. https://doi.org/10.1016/j.apgeochem.2015.08.016.

Breusch, T. S., Pagan, A. R., 1979. A Simple Test for Heteroscedasticity and Random Coefficient Variation. *Econometrica, 47*(5), 1287-1294. http://doi.org/10.2307/1911963.

Brindha, K., Elango, L., 2011. Fluoride in groundwater: causes, implications, and mitigation measures. *Fluoride properties, applications, and environmental management, 1*, 111-136.

Chiles, J.-P., Delfiner, P., 2009. Geostatistics: modeling spatial uncertainty (Vol. 497): *John Wiley & Sons*.

Chowdhury, A., Adak, M. K., Mukherjee, A., Dhak, P., Khatun, J., Dhak, D., 2019. A critical review on geochemical and geological aspects of fluoride belts, fluorosis, and natural materials, and other sources for alternatives to fluoride exposure. *Journal of Hydrology, 574*, 333-359. https://doi.org/10.1016/j.jhydrol.2019.04.033.

Cobbing, J., Hiller, B., 2019. Waking a sleeping giant: Realizing the potential of groundwater in Sub-Saharan Africa. *World Development, 122*, 597-613. https://doi.org/10.1016/j.worlddev.2019.06.024.

Cronin, S. J., Neall, V. E., Lecointre, J. A., Hedley, M. J., Loganathan, P., 2003. Environmental hazards of fluoride in volcanic ash: a case study from Ruapehu volcano, New Zealand. *Journal of Volcanology and Geothermal Research, 121*(3), 271-291. https://doi.org/10.1016/S0377-0273(02)00465-1.

Delcamp, A., Kervyn, M., Benbakkar, M., Kwelwa, S., Peter, D., 2017. Large volcanic landslide and debris-avalanche deposit at Meru Tanzania. *Landslides,* 14 (3), 833–847. https://doi.org/10.1007/s10346-016-0757-8.

Dissanayake, C. B. 1991. The fluoride problem in the groundwater of Sri Lanka — environmental management and health. *International Journal of Environmental Studies, 38*(2-3), 137-155. http://doi:10.1080/00207239108710658.

Edmunds, W. M., Smedley, P. L., 2013. Fluoride in natural waters. In *Essentials of medical geology*, (pp. 311-336): Springer.

Fawell, J., Nieuwenhuijsen, M. J., 2003. Contaminants in drinking water Environmental pollution and health. *British medical bulletin, 68*(1), 199-208.

Gaye, C. B., Tindimugaya, C., 2019. Review: Challenges and opportunities for sustainable groundwater management in Africa. *Hydrogeology Journal, 27*(3), 1099-1110. http://doi:10.1007/s10040-018-1892-1.

Ghiglieri, G., Balia, R., Oggiano, G., Pittalis, D., 2010. Prospecting for safe (low fluoride) groundwater in the Eastern African Rift: the Arumeru District (Northern Tanzania). *Hydrology and Earth System Sciences, 14*(6), 1081.

GW·MATE, 2011. Appropriate groundwater management policy for Sub-Saharan Africa in face of demographic pressure and climatic variability. World Bank Strategic Overview Series no. 5. *World Bank*, Washington, DC. https://www.researchgate.net/publication/284454169.

HACH, 2021. Fluoride, ISE Method for Drinking Water: www.hach.com.

Haining, R., Wise, S., Ma, J. 1998. Exploratory spatial data analysis. *Journal of the Royal Statistical Society: Series D (The Statistician), 47*(3), 457-469.

Hoch, J. S., 2012. A Review of: "Econometric Analysis, Seventh Edition, by W. H. Greene". *Journal of Biopharmaceutical Statistics, 22*(5), 1081-1083. http://doi:10.1080/10543406.2012.701589.

Ijumulana, J., Ligate, F., Bhattacharya, P., Mtalo, F., Zhang, C., 2020. Spatial analysis and GIS mapping of regional hotspots and potential health risk of fluoride concentrations in groundwater of northern Tanzania. *Science of The Total Environment*, 139584. https://doi.org/10.1016/j.scitotenv.2020.139584.

Ijumulana, J., Ligate, F., Irunde, R., Bhattacharya, P., Maity, J. P., Ahmad, A., Mtalo, F., 2021. Spatial uncertainties in fluoride levels and health risks in endemic fluorotic regions of northern Tanzania. *Groundwater for Sustainable Development, 14*, 100618. https://doi.org/10.1016/j.gsd.2021.100618.

Jacks, G., Bhattacharya, P., Chaudhary, V., Singh, K. P., 2005. Controls on the genesis of some high fluoride groundwaters in India. *Applied Geochemistry, 20*(2), 221-228. https://doi.org/10.1016/j.apgeochem.2004.07.002.

Jarque, C. M., Bera, A. K., 1980. Efficient tests for normality, homoscedasticity, and serial independence of regression residuals. *Economics Letters, 6*(3), 255-259.

Kimambo, V., Bhattacharya, P., Mtalo, F., Mtamba, J., Ahmad, A., 2019. Fluoride occurrence in groundwater systems at global scale and status of defluoridation – State of the art. *Groundwater for Sustainable Development, 9*, 100223. https://doi.org/10.1016/j.gsd.2019.100223.

Kisaka, M., Fontijn, K., Shemsanga, C., Tomašek, I., Gaduputi, S., Debaille, V., Delcamp, A., Kervyn, M., 2021. The late Quaternary eruptive history of Meru volcano, northern Tanzania. Journal of Volcanology and Geothermal Research, 417, 107314. https://doi.org/https://doi.org/10.1016/j.jvolgeores.2021.107314

Koenker, R., Bassett Jr, G., 1982. Robust tests for heteroscedasticity based on regression quantiles. *Econometrica: Journal of the Econometric Society*, 43-61.

Lapworth, D. J., MacDonald, A. M., Kebede, S., Owor, M., Chavula, G., Fallas, H., Wilson, P. R., Ward, J., Lark, M., Okullo, J., 2020. Drinking water quality from rural handpump boreholes in Africa. *Environmental Research Letters*. *5*(6), 064020. https://doi.org/10.1088/1748-9326/ab8031.

Ligate, F., Ijumulana, J., Ahmad, A., Kimambo, V., Irunde, R., Mtamba, J.O., Mtalo, F., Bhattacharya, P., 2021 Groundwater resources in the East African Rift Valley: Understanding the geogenic contamination and water quality challenges in Tanzania. *Scientific African* https://doi.org/10.1016/j.sciaf.2021.e00831 (In Press)

MacDonald, A. M., Bonsor, H. C., Dochartaigh, B. É. Ó., & Taylor, R. G., 2012. Quantitative maps of groundwater resources in Africa. *Environmental Research Letters*, 7(2), 024009. https://doi.org/10.1088/1748-9326/7/2/024009.

MacDonald, A. M., Calow, R. C., 2009. Developing groundwater for secure rural water supplies in Africa. *Desalination*, 248(1), 546-556. https://doi.org/10.1016/j.desal.2008.05.100.

Maity, J. P., Vithanage, M., Kumar, M., Ghosh, A., Mohan, D., Ahmad, A., Bhattacharya, P., 2021. Seven 21st century challenges of arsenic-fluoride contamination and remediation. *Groundwater for Sustainable Development*, 12, 100538. https://doi.org/10.1016/j.gsd.2020.100538.

Mohanta, A., Mohanty, P. K., 2018. Dental Fluorosis-Revisited. *Biomedical Journal of Scientific & Technological Research, 2*(1). http://doi:10.26717/BJSTR.2018.02.000667.

Moran, P. A., 1950. Notes on continuous stochastic phenomena. *Biometrika*, *37*(1/2), 17-23. http://doi.org/10.2307/2332142.

Mridha, D., Priyadarshni, P., Bhaskar, K., Gaurav, A., De, A., Das, A., Joardar, M., Chowdhury, N. R., Roychowdhury, T., 2021. Fluoride exposure and its potential health risk assessment in drinking water and staple food in the population from fluoride endemic regions of Bihar, India. *Groundwater for Sustainable Development, 13*, 100558. https://doi.org/10.1016/j.gsd.2021.100558.00000.

NBS, 2018. Tanzania in Figures 2017. National Bureau of Statistics, Dar es Salaam, The United Republic of Tanzania 105p. https://www.nbs.go.tz/index.php/en/tanzania-in-figures/433-tanzania-in-figures-2017.

Pavelic P, Giordano M, Keraita B, Ramesh V, Rao T. (eds), 2012. Groundwater availability and use in Sub-Saharan Africa: A review of 15 countries. Colombo, Sri Lanka: *International Water Management Institute (IWMI).* p 274. https://doi.org/10.5337/ 2012.213.

Shivaprakash, P., Ohri, K., Noorani, H., 2011. Relation between dental fluorosis and intelligence quotient in school children of Bagalkot district. *Journal of Indian Society of Pedodontics and Preventive Dentistry, 29*(2), 117.

Symanzik, J., 2014. Exploratory Spatial Data Analysis. In M. M. Fischer P. Nijkamp (Eds.), *Handbook of Regional Science* (pp. 1295-1310). Berlin, Heidelberg: Springer Berlin Heidelberg.

Solomon, D., Lehmann, J., Zech, W., 2000. Land-use effects on soil organic matter properties of chromic luvisols in semi-arid northern Tanzania: carbon, nitrogen, lignin, and carbohydrates. *Agriculture, Ecosystems & Environment, 78*(3), 203-213. https://doi.org/10.1016/S0167-8809(99)00126-7.

Susheela, A. K., Bhatnagar, M., 2002. Reversal of fluoride induced cell injury through elimination of fluoride and consumption of diet rich in essential nutrients and antioxidants. In V. Vallyathan, X. Shi, & V. Castranova (Eds.), *Oxygen/Nitrogen Radicals: Cell Injury and Disease* (pp. 335-340). Springer US. https://doi.org/10.1007/978-1-4615-1087-1_38

Tomašek, I., Mouri, H., Dille, A., Bennett, G., Bhattacharya, P., Brion, N., Elskens, M., Fontijn, K., Gao, Y., Gevera, P. K., Ijumulana, J., Kisaka, M., Leermakers, M., Shemsanga, C., Walraevens, K., Wragg, J., Kervyn, M., 2021. Naturally occurring potentially toxic elements in groundwater from the volcanic landscape around Mount Meru, Arusha, Tanzania and their potential health hazard. *Science of The Total Environment*, 150487. https://doi.org/https://doi.org/10.1016/j.scitotenv.2021.150487

Vithanage, M., Bhattacharya, P., 2015. Fluoride in the environment: sources, distribution, and defluoridation. *Environmental Chemistry Letters*, 13(2), 131-147. http://doi:10.1007/s10311-015-0496-4.

Water Quality Service Division, Ministry of Water (MoW), 2016. Mapping of fluoride levels in Water sources in Arusha, Manyara, Kilimanjaro, Shinyanga, Singida, and Mwanza, Tanzania (*Unpublished*).

Wilkinson, P., Mitchell, J.G., Cattermole, P.J., Downie, C., 1986. Volcanic chronology of the Meru-Kilimanjaro region, Northern Tanzania. *Journal of Geological Society*. 143 (4), 601–605. https://doi.org/10.1144/gsjgs.143.4.0601.

WHO, 2011. Guidelines for drinking-water quality, Fourth Edition, *WHO chronicle, 38*(4), 104-108.

WHO, 2017. Guidelines for drinking-water quality: the fourth edition incorporating the first addendum. Geneva: Licence: CC BY-NC-SA 3.0 IGO.

Yasrebi, J., Saffari, M., Fathi, H., Karimian, N., Moazallahi, M., Gazni, R., 2009. Evaluation and comparison of ordinary kriging and inverse distance weighting methods for prediction of spatial variability of some soil chemical parameters. *Research Journal of Biological Sciences, 4*(1), 93-102.

List of Figures

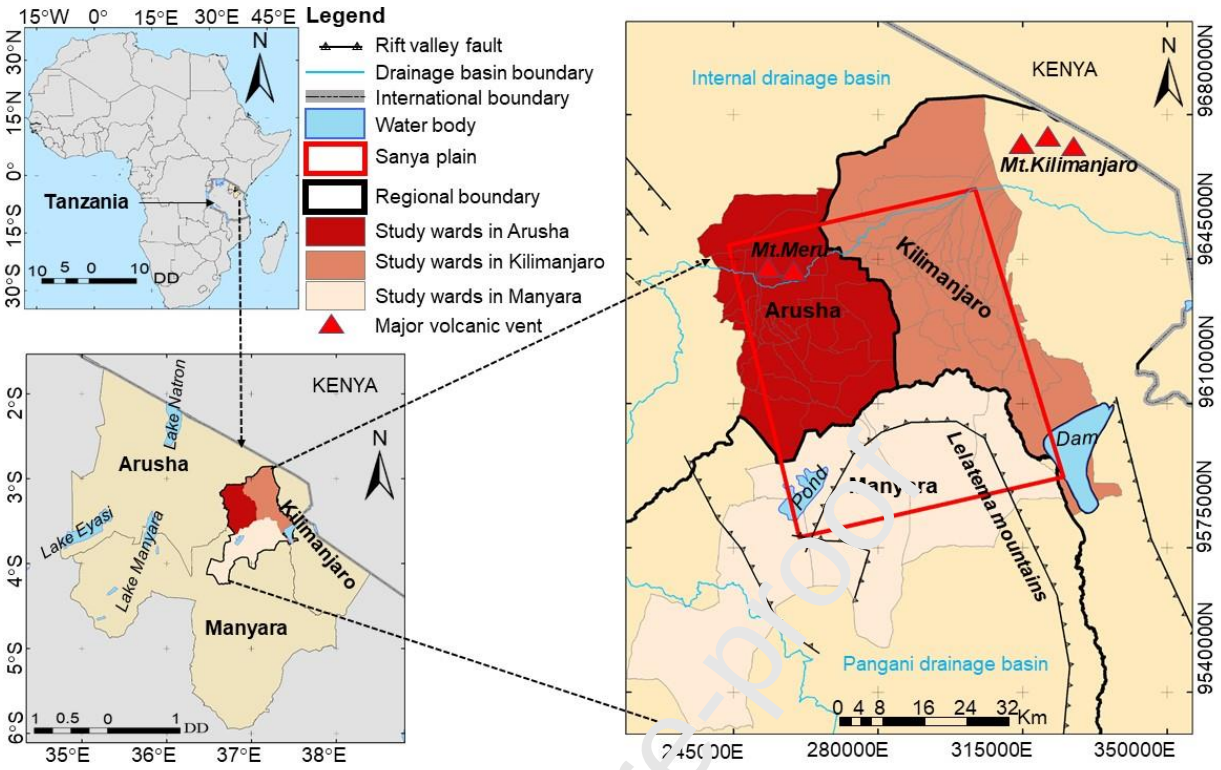

Figure 1: Location map of Sanya alluvial plain in the northern development zone of Tanzania within the East African Rift Valley graben (The spatial extent of the Sanya plain was estimated from standard Topographical maps at 1: 50,000 scale obtained from the Survey and Mapping Department (Table 1)).

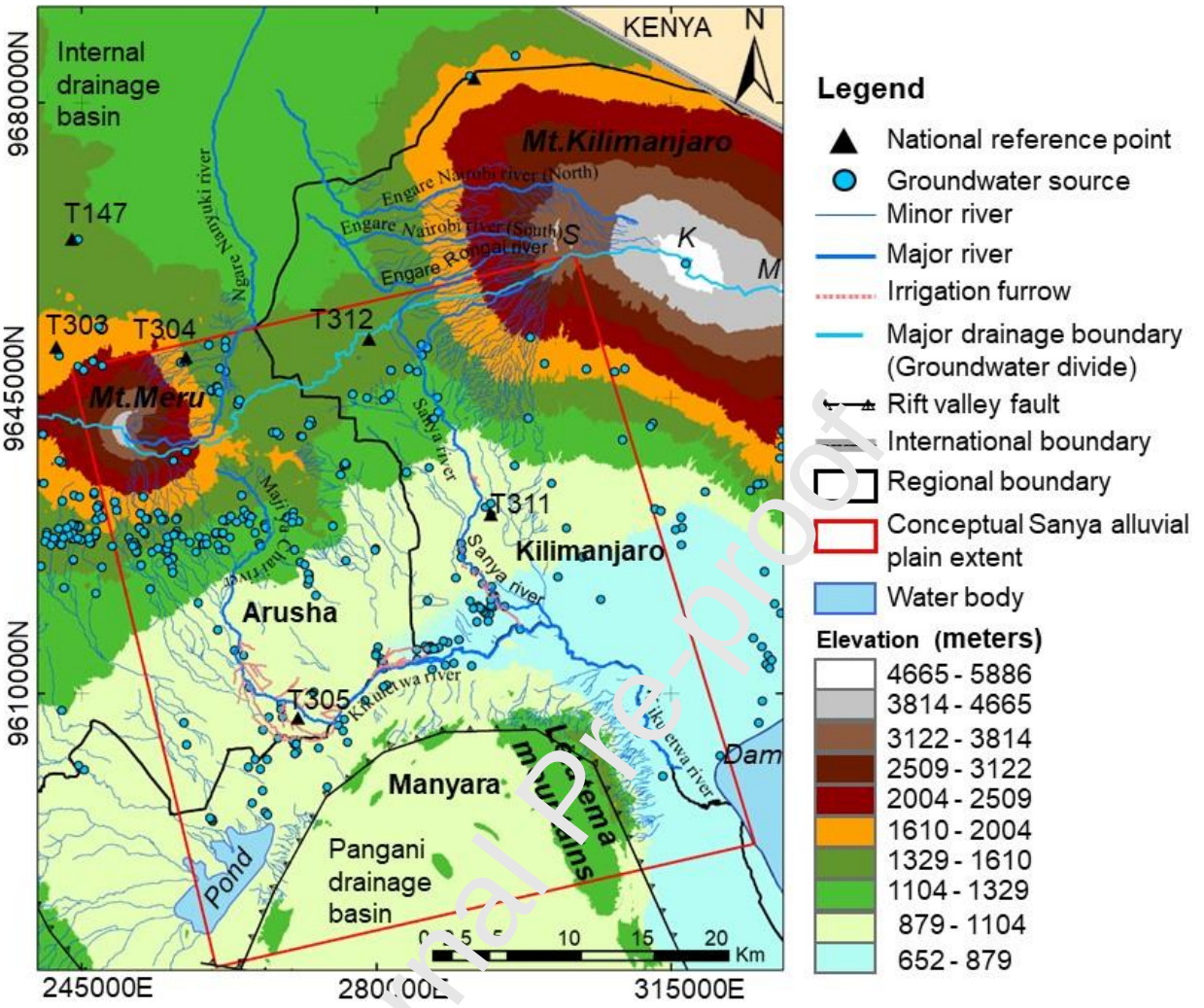

Figure 2: General relief map of Sanya alluvial plain in the graben between Mt. Meru, Mt. Kilimanjaro in the northwest and northeast, respectively, and the Lelatema mountains in the south.

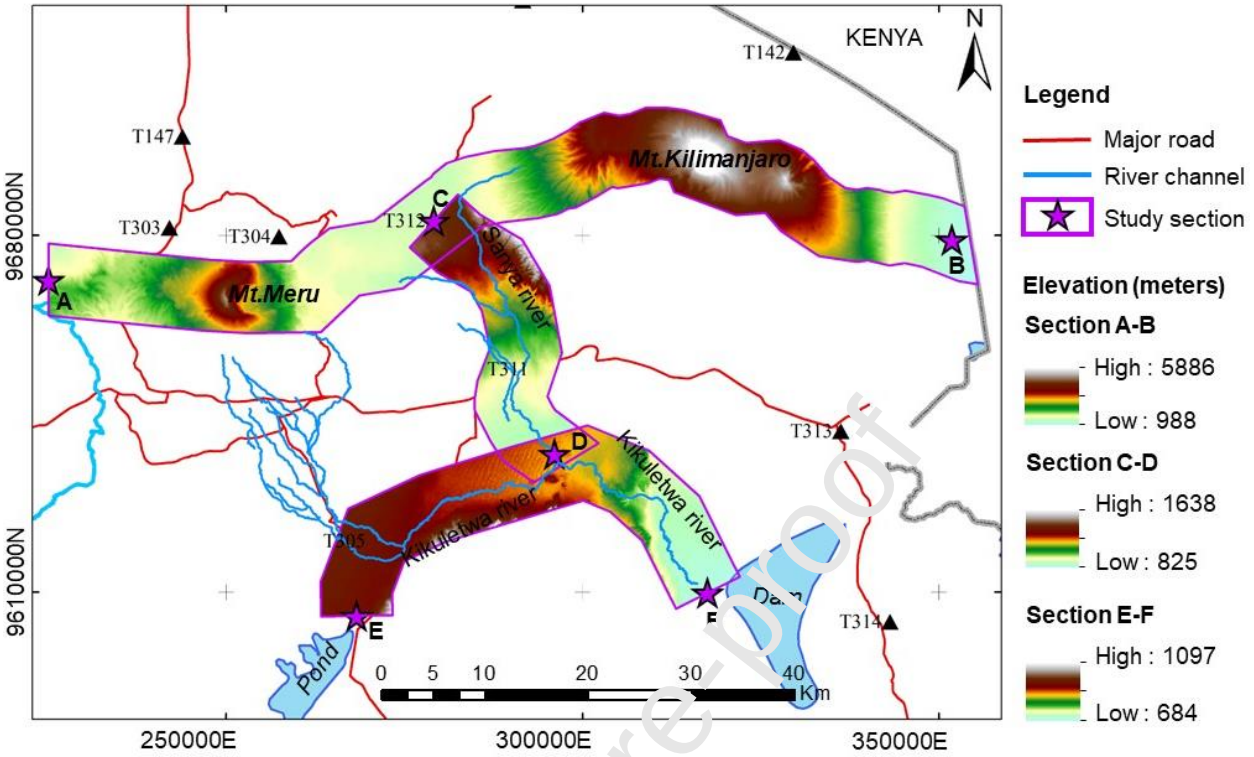

Figure 3: Conceptual hydrogeological study sections of the sources and mobilization of fluoride in the Sanya alluvial plain (a) along the groundwater divide in the north (Section A-B), (b) along Sanya river valley (Section C-D), and (c) across Sanya plain in the south (Section E-F).

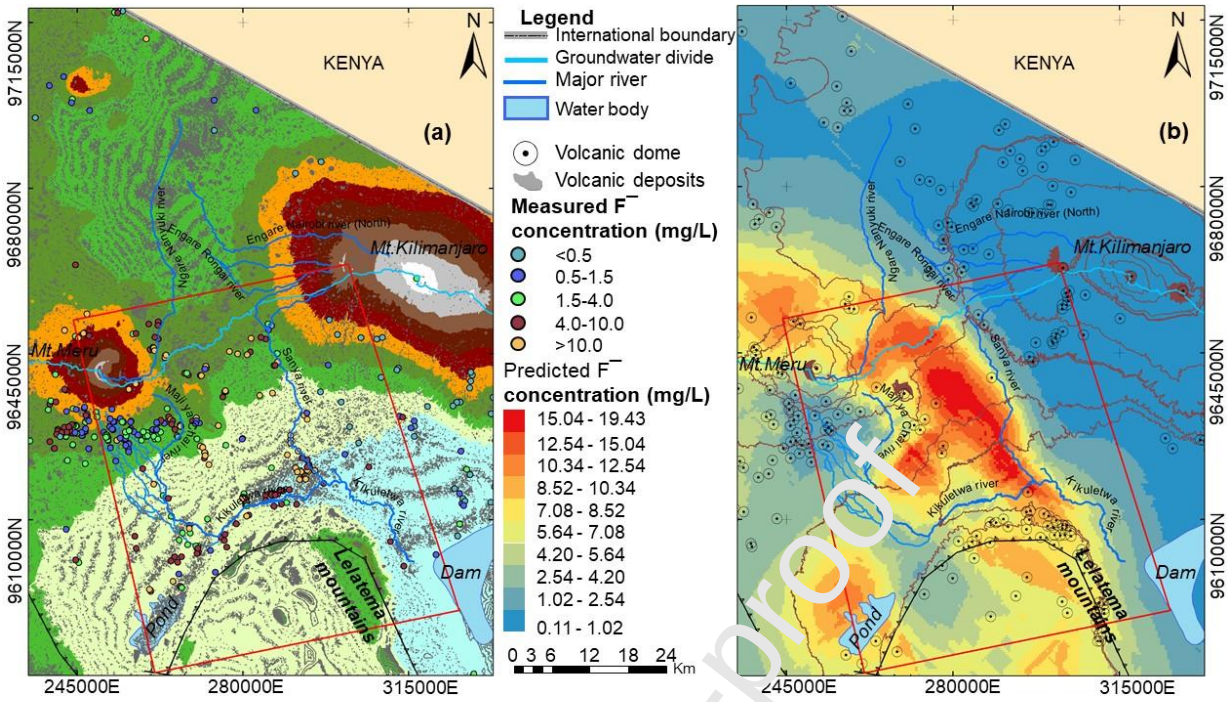

Figure 4:(a)Statistical and (b) spatial distribution of fluoride concentration in groundwater sources around Sanya alluvial plain.

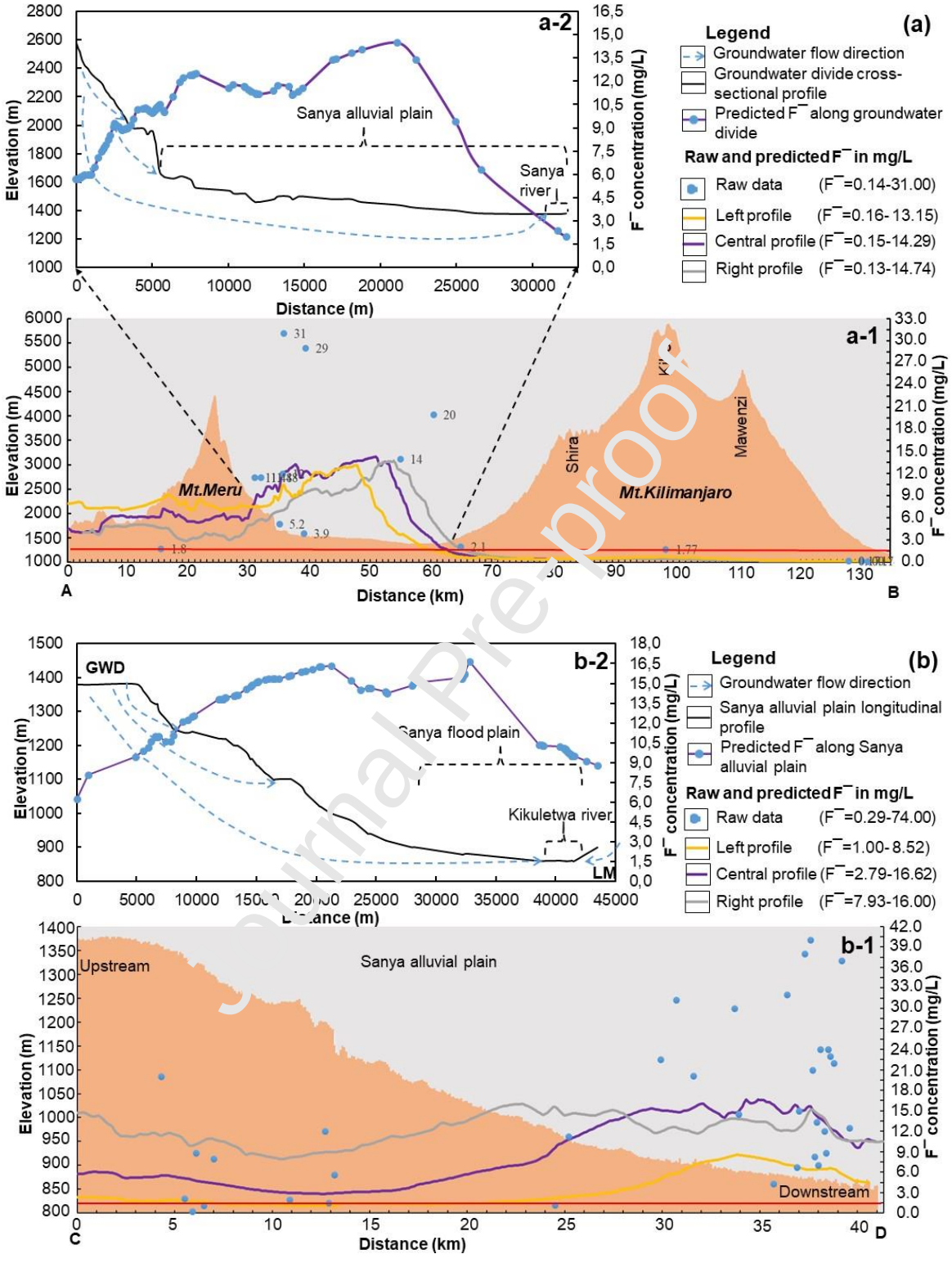
(a)
a-2
Legend
Groundwater flow direction
Groundwater divide cross-sectional profile
Predicted F⁻ along groundwater divide
Raw and predicted F⁻ in mg/L
Raw data (F⁻=0.14-31.00)
Left profile (F⁻=0.16- 13.15)
Central profile (F⁻=0.15-14.29)
Right profile (F⁻=0.13-14.74)
Sanya alluvial plain
Sanya river
Elevation (m)
F⁻ concentration (mg/L)
Distance (m)
a-1
Mt.Meru
Mt.Kilimanjaro
Shira
Mawenzi
A
B
Distance (km)
(b)
b-2
GWD
Legend
Groundwater flow direction
Sanya alluvial plain longitudinal profile
Predicted F⁻ along Sanya alluvial plain
Raw and predicted F⁻ in mg/L
Raw data (F⁻=0.29-74.00)
Left profile (F⁻=1.00- 8.52)
Central profile (F⁻=2.79-16.62)
Right profile (F⁻=7.93-16.00)
Sanya flood plain
Kikuletwa river
LM
b-1
Upstream
Sanya alluvial plain
Downstream
C
D
Distance (km)

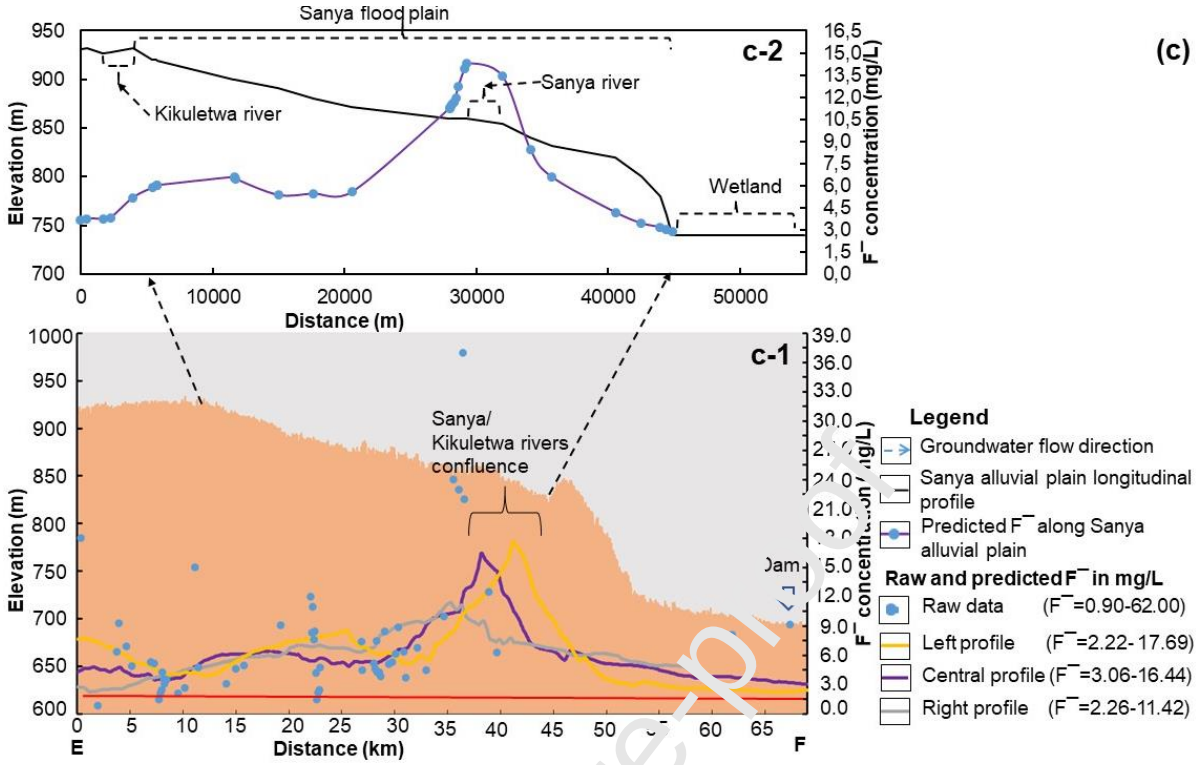

Figure 5: The variation of fluoride concentrations within Sanya plain (a) across the Sanya plain at the start of the plain between Mt. Meru and Kilimanjaro-Section A-B, (b) along Sanya river valley from the groundwater divide (GWD) in the north to the south in the floodplain-Section C-D and (c) across Sanya floodplain along Kikuletwa river which acts as the regional boundary between Manyara and Arusha region-Section E-F.

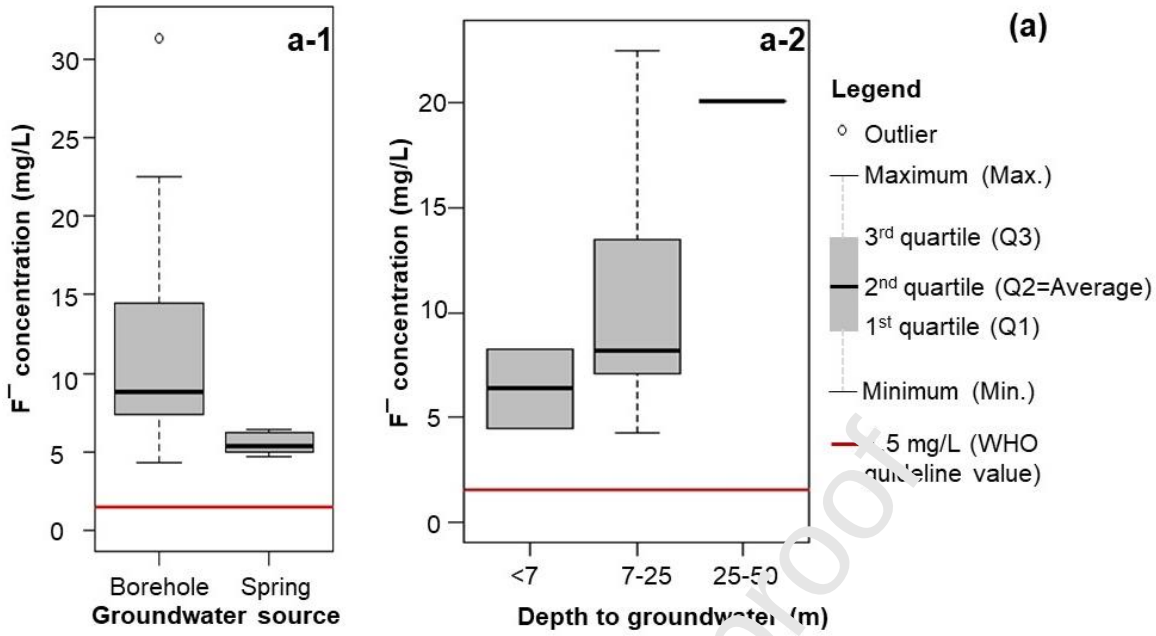

Groundwater Source	F⁻ concentration (mg/L)							
	Min.	Max.	Q1	Median	Q3	IQR	Mean	s.d
Borehole	4.29	31.25	8.28	12.90	20.10	11.82	14.23	8.27
Spring	4.70	6.46	5.02	5.39	6.25	1.23	5.55	0.65

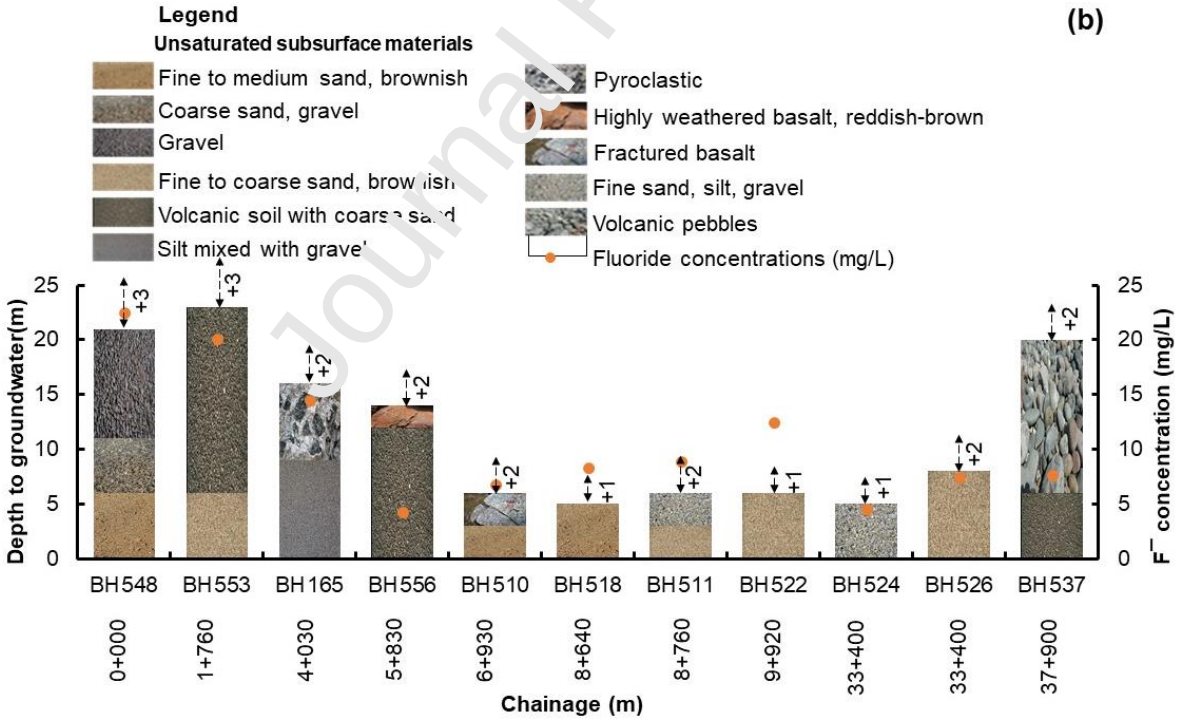

Figure 6: (a) Statistical distribution of fluoride concentrations in groundwater sources and (b) spatial variability of depth to groundwater and unsaturated subsurface sediments in the Sanya/Kikuletwa flood plain.

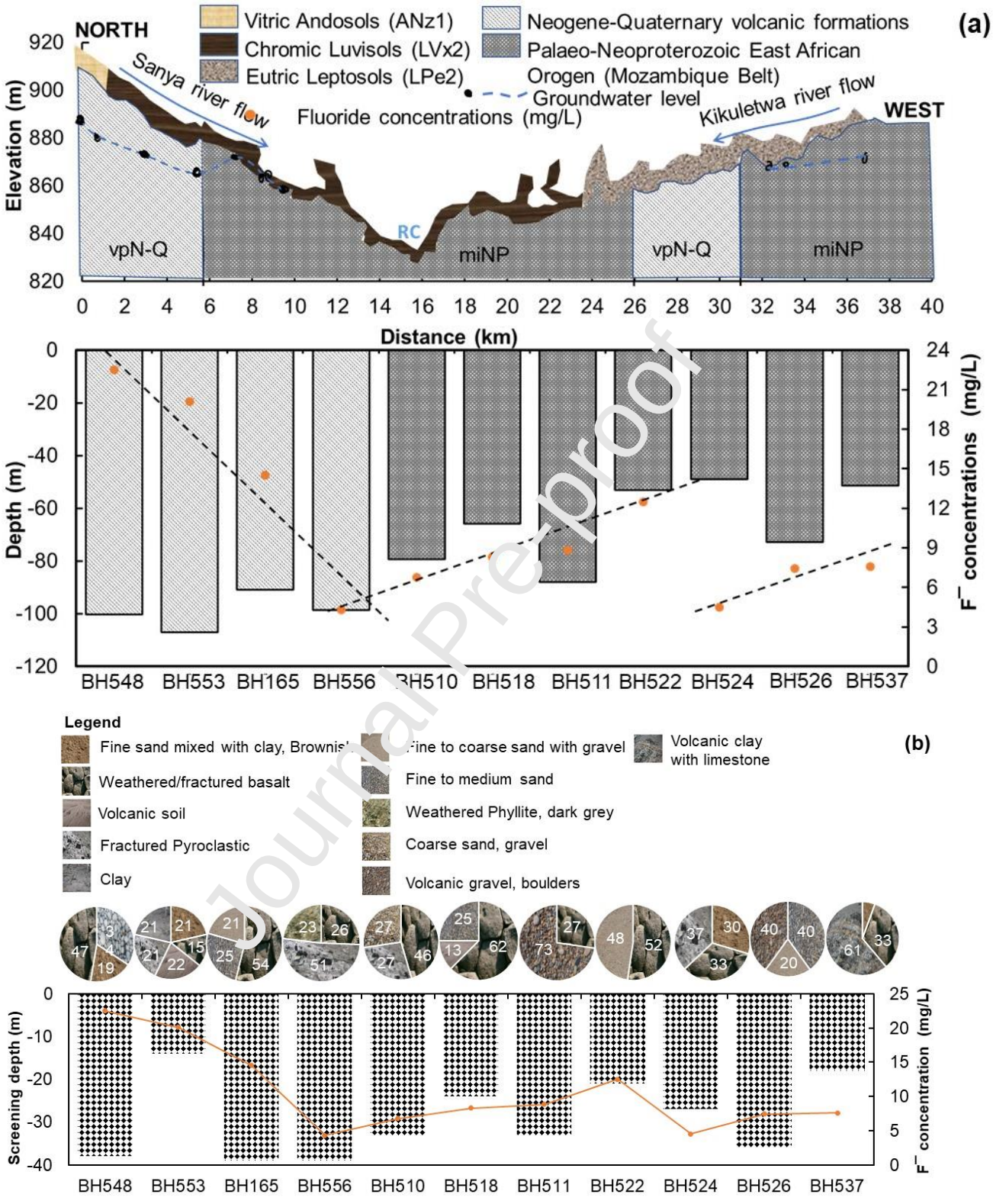

Figure 7: Spatial variability of fluoride concentrations with (a) depth in different soil and rock formations and (b) screening depth with different degrees of aquifer materials along Sanya and Kikuletwa rivers within the Sanya alluvial flood plain in northern Tanzania.

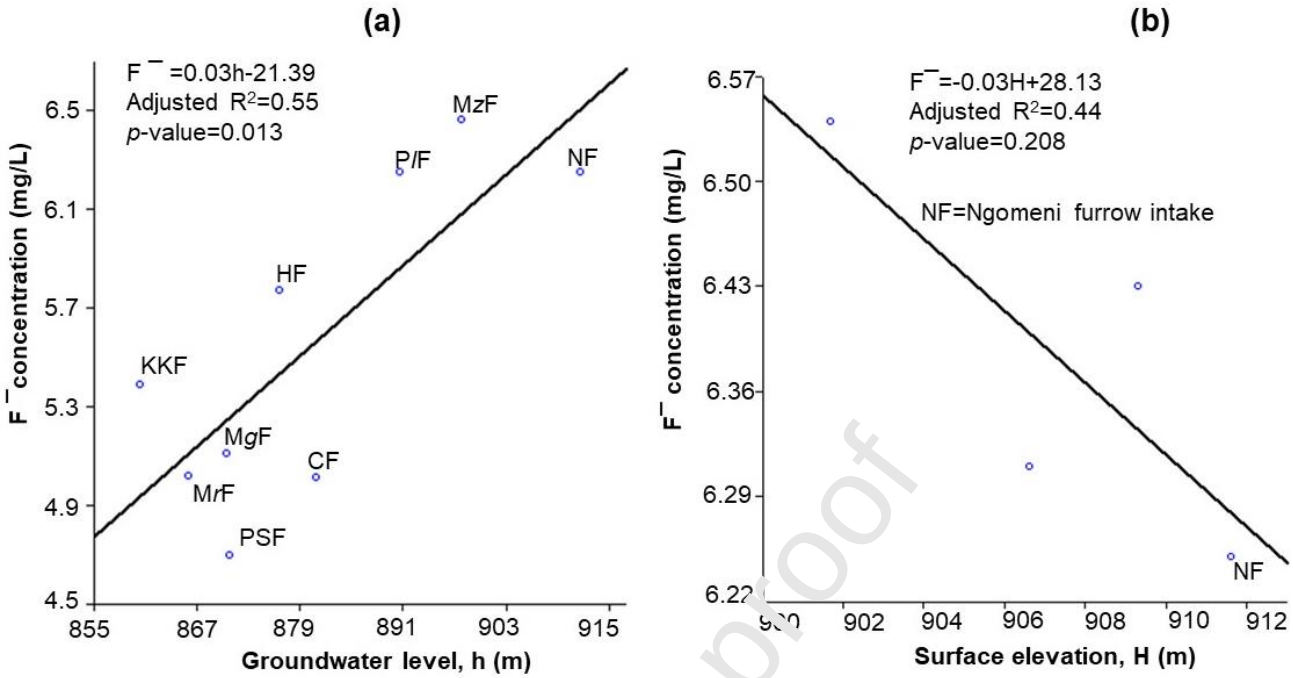

Figure 8: Variation of fluoride concentrations along Sanya river. Water samples collected from Ngomeni furrow (NF), Mzegazega furrow (MzF), Palestina furrow (PlF), Hemed furrow (HF), Migungani furrow (MgF), Cement furrow (CF), Mrinji furrow (MrF), Peter Sechu furrow (PSF) and Kitivo Kati furrow (KKF).

List of Tables

Table 1: Spatial data sources and types used in this study.

Spatial data source	Spatial data type description
Pangani Basin Water Office (PBWO)	• Completed drilling reports of 14 boreholes in the Sanya floodplain. The boreholes were drilled in the year 2011 to support irrigation activities in the Sanya floodplain during the dry season. • Major drainage basin boundaries (Pangani and Internal drainage basin).
National Bureau of Statistics (NBS) of the United Republic of Tanzania (URT)	• Regional, district, and ward boundaries as well as population data based on 2012 census reports.
Global digital elevation model (GDEM)	• Free open-source elevation data (30 m resolution) downloaded from https://gisdata.mn.gov/dataset/elev-30m-digital-elevation-model.
Survey and Mapping Division of the Ministry of Lands, Housing and Human Settlements Development (SMD MLHHSD)	• Coordinates for national control points, particularly, T305, T311, and T312. • Standard topographical maps at 1:50,000 scale: Sanya Chini (Sheet no. 56/3), West Hai (Sheet no.56/1, Ngare Nanyuki (Sheet no.55/2), Ngasurai (Sheet no.41/4), Usa River (Sheet no.55/4), Mbuguni (Sheet no. 71/2), Lossoito (Sheet no. 72/1), and Arusha Chini (Sheet no. 72/2).
Open source DivaGIS portal	• Shapefiles for African country boundary downloaded at Free Spatial Data | DIVA-GIS (diva-gis.org).
Field surveys in northern Tanzania	• F^- concentrations from 14 boreholes and 9 springs during fieldwork campaign between 2018 and 2020. • Surface elevations for the 14 boreholes and 9 springs along the Sanya river channel.

Table 2: OLS estimates

Variable	Coefficient	Std. Error	t-Statistic	Probability
Constant	25.828	7.96606	3.24226	0.01764
Depth to groundwater	1.38238	0.242201	5.70756	0.00125
Borehole depth	-0.39389	0.117776	-3.34441	0.01553
Screen depth	0.0371908	0.145018	0.256456	0.80617

Table 3: OLS regression model diagnostics

Test #	Test name	Degrees of freedom (df)	Value	Probability
1	Jarque-Bera	3	0.2770	0.87066
2	Breusch-Pagan	2	3.5854	0.20480
3	Koenker-Bassett	2	4.3974	0.22163

Graphical Abstract

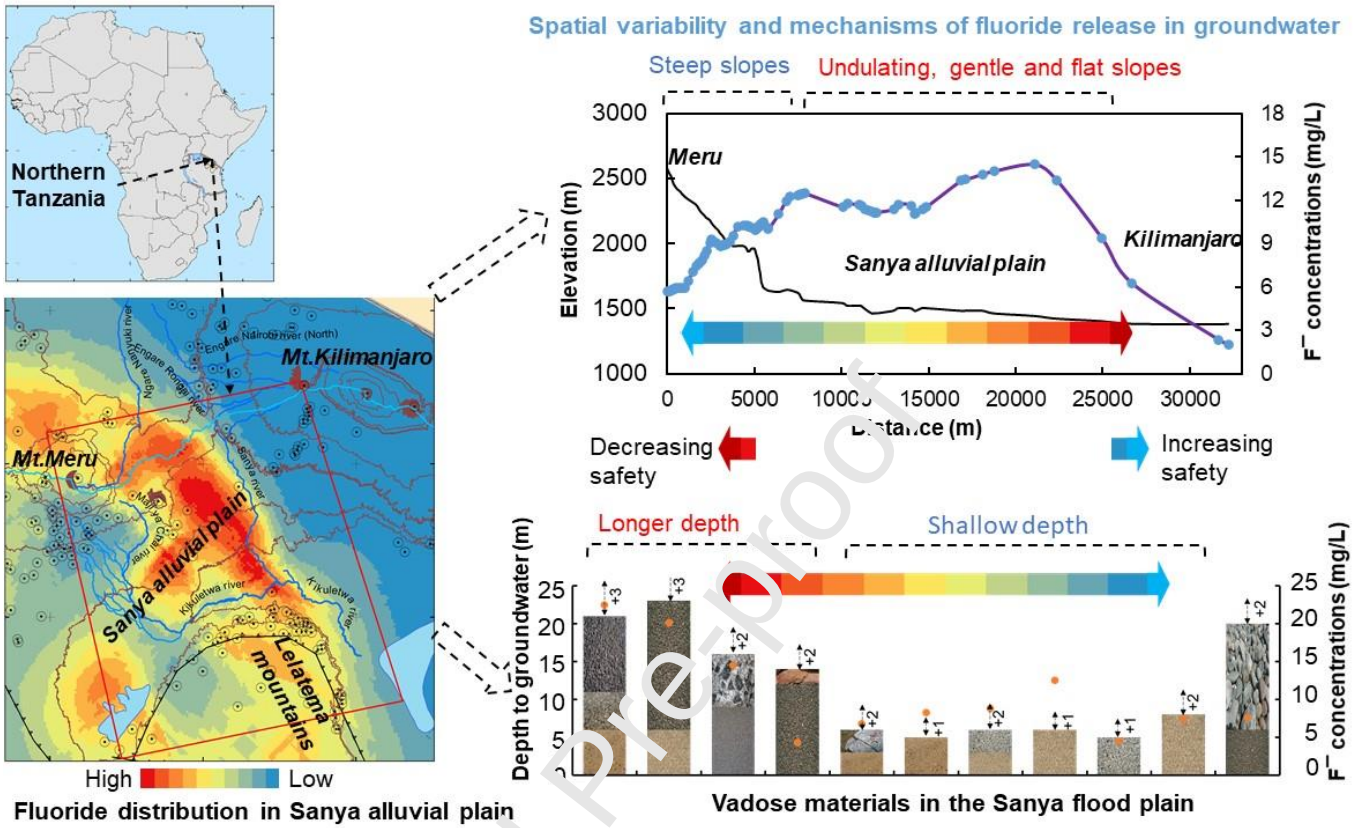

Highlights

- Debris-avalanche deposits dynamics trigger the widespread of fluoride in groundwater.
- Depth to groundwater enhances the variability of fluoride in volcanic aquifers.
- Safe groundwater for drinking purposes exists at steep slopes of stratovolcanoes.
- Deep fractured aquifers are potential sources of safe fluoride water.
- Irrigation agriculture enhances the variability of fluoride in shallow aquifers.